Semi-Blind Estimation of Correlated MIMO Channels using Optimal Training Design in Multiuser Environments

Office of Naval Research (ONR) Grant N00014-10-1-0065

Srikanth Pagadarai and Alexander M. Wyglinski
Department of Electrical and Computer Engineering
Worcester Polytechnic Institute
Worcester, MA, 01609 USA
E-mail: {srikanthp, alexw}@ece.wpi.edu

Christopher R. Anderson
Department of Electrical Engineering
United States Naval Academy
Annapolis MD, 21402 USA
E-mail: canderso@usna.edu

January 27, 2011

Chapter 1

Introduction

1.1 Project Scope

With the increasing volume of wireless traffic that theatre operations require, the probability of transmissions interfering with each other is steadily growing to the point that new techniques need to be employed. Furthermore, to combat remotely operated improvised explosive devices, many ground convoys transmit high-power broadband jamming signals, which blocks both hostile as well as friendly communications. These wideband jamming fields pose a serious technical challenge to existing anti-jamming solutions that are currently employed by the Navy and Marine Corps. The outcomes of the proposed project will help enable reliable communications given these new challenges given a network partially composes of legacy systems.

We propose to devise, implement, and evaluate an adaptive signal processing software solution for mitigating the effects of both intentional and unintentional jamming (including wideband jamming) via the combination of antenna subset selection, spectral subtraction, and blind source separation (BSS) techniques in order to extract specific transmissions from a mixture of intercepted wireless signals. The goal of our proposed solution, called BLInd Spectrum Separation (BLISS), is to enable reliable, high throughput, and robust end-to-end wireless communications in the support of all Department of Navy missions, especially high capacity multimedia (voice, data, imagery) transmissions. In particular, the focus of our proposed work is the so-called "disadvantaged user", e.g., small-deck combatants, submarines, unmanned air vehicles (UAVs), dispersed ground units in urban and radio frequency (RF) challenged environments. For instance, the evaluation of the BLISS software will be conducted on a TALON platform at the U.S. Naval Academy operating in a wideband jamming field.

The scenario specifically addressed by this proposed project is shown in Figure 1.1, where a Navy/Marines communication network consisting of several disadvantaged users and employing the BLISS algorithm is operating in the presence of a wideband jamming signal that is intentionally generated by one of the users. By employing the BLISS software in conjunction with a receive antenna array, individual wireless transmissions of interest can be separated into their individual components while the jamming signal is rejected.

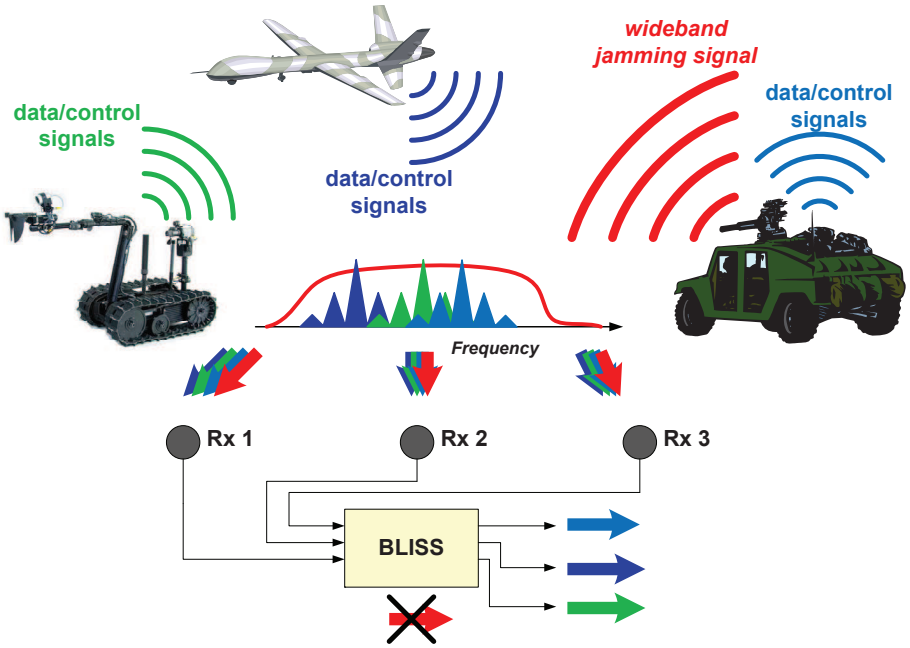

Figure 1.1: Overview of the proposed BLISS framework for achieving jamming immunity. Notice how the spectrally-overlapping data/control signals are separated by BLISS in the presence of a wideband jamming signal (the latter is discarded by BLISS)

1.2 Project Objectives

The primary technical objectives of the proposed project are as follows:

- Development of an adaptive signal processing software solution combining antenna subset selection, spectral subtraction, and blind source separation (i.e., BLISS) that can mitigate the impact of both wideband jamming and co-site interference by extracting individual transmissions from multiple intercepted mixtures of wireless signals.
- Implementation of the BLISS software as a collection of several signal processing blocks employed by an existing SDR architecture, e.g., GNU Radio, SCA.
- Operational assessment of the performance of SDR platforms employing the BLISS software in both a controlled laboratory environment as well as in field experiments using actual hardware platforms (e.g., TALON robots). The processing capabilities required by the SDR platforms to employ the BLISS software will also be evaluated in order to determine which platforms are best-suited for this solution.

Chapter 2

Current Project Status by Technical Tasks

Given this technically challenging project, the WPI/USNA joint research team has made several important achievements during this project with respect to several of the proposed subtasks, including a theoretical framework for performing blind source separation of multiple wireless signals and the creation of an antenna subset selection (AntSS) hardware module prototype. However, there were several factors and events that were completely beyond the control of the project PIs, thus resulting in significant delays. These factors and events include:

- A 3-month delay in accepting funds due to CRADA execution.
- A 1-year delay in hiring a post-doctoral researcher at the USNA due to logistical difficulties at the USNA Comptroller Office.
- The forced medical leave of PI Anderson for 3 months.

Consequently, despite the best efforts of the WPI/USNA joint research team, the completion of the specified subtasks have been delayed on the order of several months. As a result, the current status of each subtask is as follows:

- Technical Task I - Adaptive Signal Processing Algorithm Development:
  - **Subtask A - Implement Spectral Subtraction Algorithm:** Once Subtask C has been completed, the WPI research team will perform this subtask during Summer 2011 and complete it by August 2011.
  - **Subtask B - Devise Wireless Channel Mixing Model:** This subtask was completed early on in the project, yielding an accurate channel mixing model that closely matches the wireless environment in which the BLISS prototype system will operate. The resulting model was subsequently employed in Subtask C.
  - **Subtask C - Implement Blind Source Separation Algorithm:** The majority of this subtask has been completed, include the entire system model. However, there are still several additional enhances that need to be made in order to ensure

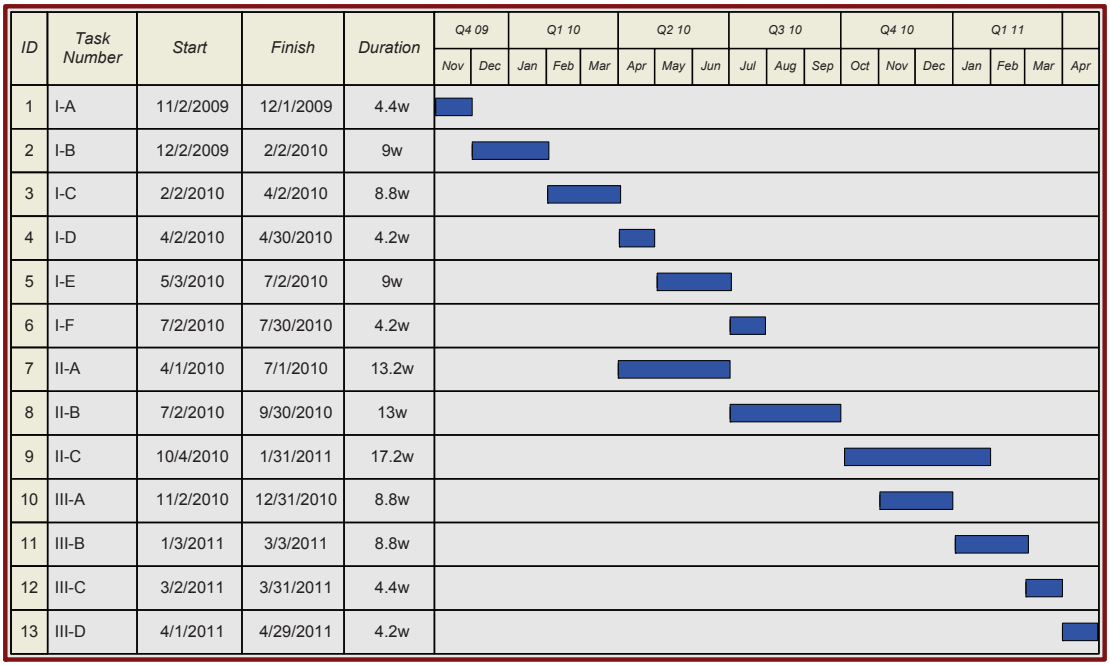

ID	Task Number	Start	Finish	Duration
1	I-A	11/2/2009	12/1/2009	4.4w
2	I-B	12/2/2009	2/2/2010	9w
3	I-C	2/2/2010	4/2/2010	8.8w
4	I-D	4/2/2010	4/30/2010	4.2w
5	I-E	5/3/2010	7/2/2010	9w
6	I-F	7/2/2010	7/30/2010	4.2w
7	II-A	4/1/2010	7/1/2010	13.2w
8	II-B	7/2/2010	9/30/2010	13w
9	II-C	10/4/2010	1/31/2011	17.2w
10	III-A	11/2/2010	12/31/2010	8.8w
11	III-B	1/3/2011	3/3/2011	8.8w
12	III-C	3/2/2011	3/31/2011	4.4w
13	III-D	4/1/2011	4/29/2011	4.2w

Figure 2.1: Initially proposed time line at the beginning of this project.

a robust implementation. Moreover, the feedback suggested by the reviewers of the conference paper based on this subtask (see Appendix A) will be incorporated in this implementation. This subtask should be completed by April 2011, with a revision of [1] submitted to the 2011 IEEE Global Telecommunications Conference, as well as an expanded version submitted as a journal paper to the IEEE Transactions on Signal Processing.

– **Subtask D - Devise Antenna Subset Selection Algorithm:** The USNA research team devised an AntSS hardware solution for this subtask, which will interface directly to the USRP2 software-defined radio platforms employed in the experimentation phase of this project. At present, the AntSS boards are currently being tested, and should be fully operational by May 2011. The results of this subtask will be submitted for publication to the 2011 Military Communications Conference, with an expanded version of this paper submitted to the IEEE Transactions on Wireless Communications.

– **Subtask E - Combine Blind Signal Separation, Spectral Subtraction, and Antenna Subset Selection Algorithms:** This subtask will be performed during Summer 2011 once Subtask C and Subtask D have been completed, and Subtask A is being conducted. It is expected that this subtask will be completed by August 2011.

– **Subtask F - Evaluation of Integrated BLISS Framework:** As functional prototype subcomponents of this project are gradually being implemented, they are being tested and the compatibility of each subcomponent is evaluated. However, the majority of this subtask will be completed once Subtask A, Subtask C,

and Subtask D have been completed or are close to completion.

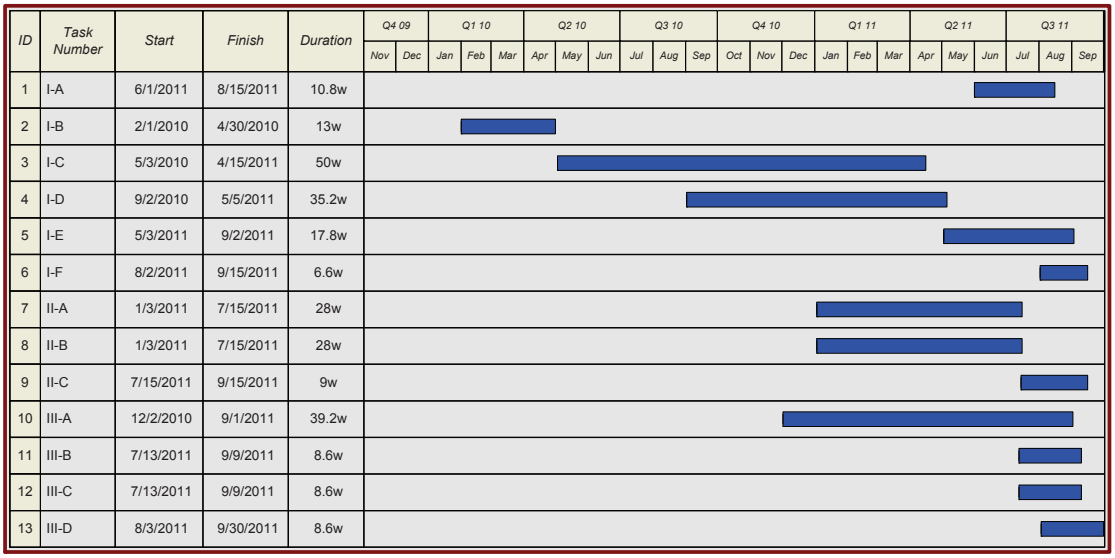

ID	Task Number	Start	Finish	Duration
1	I-A	6/1/2011	8/15/2011	10.8w
2	I-B	2/1/2010	4/30/2010	13w
3	I-C	5/3/2010	4/15/2011	50w
4	I-D	9/2/2010	5/5/2011	35.2w
5	I-E	5/3/2011	9/2/2011	17.8w
6	I-F	8/2/2011	9/15/2011	6.6w
7	II-A	1/3/2011	7/15/2011	28w
8	II-B	1/3/2011	7/15/2011	28w
9	II-C	7/15/2011	9/15/2011	9w
10	III-A	12/2/2010	9/1/2011	39.2w
11	III-B	7/13/2011	9/9/2011	8.6w
12	III-C	7/13/2011	9/9/2011	8.6w
13	III-D	8/3/2011	9/30/2011	8.6w

Figure 2.2: Revised time line based on current progress towards project deliverables.

- Technical Task II - Software-Defined Radio Implementation:
  - **Subtask A - Algorithm Translation to High-Level Programming Language:** This subtask commenced in January 2011 and should be completed sometime around July 2011.
  - **Subtask B - Application to Software-Defined Radio Platform:** This subtask commenced in January 2011 and should be completed sometime around July 2011.
  - **Subtask C - Algorithm Evaluation in Emulated Mixing Environment:** Once all the subtasks of Technical Task I have been completed, or are close to completion, and the fundamental software-defined radio code base devised in Subtask A and Subtask B have been implemented, the evaluation of the algorithms will be performed to ensure that their operational behavior is stable.
- Technical Task III - BLISS Hardware Prototype Demonstration:
  - **Subtask A - Physical Interface of BLISS-Enabled Software-Defined Radios with TALON Platforms:** This subtask commenced in December 2010 and should be completed sometime around September 2011.
  - **Subtask B - Formulation of End-to-End Data Communications:** This subtask will commence during Summer 2011 and completed by September 2011.
  - **Subtask C - Operation of TALON Platform under Ideal Conditions:** This subtask will commence during Summer 2011 and completed by September 2011.

– **Subtask D - Evaluation of BLISS-Enabled TALON Platforms in Wideband Jamming Fields:** This subtask will commence during Summer 2011 and completed by September 2011.

Regarding revisions to the initially proposed project time line (see Figure 2.1), we have updated the scheduled completion of the proposed subtasks and illustrated them in the time line shown in Figure 2.2. Of particular importance, the research team is expecting to complete a fully functional AntSS hardware module that can interface with USRP2 devices as well as completed blind source separation algorithm by the NRL Comms Gathering in May 2011. Furthermore, with the rest of the subtasks completed throughout Summer 2011, the WPI/USNA research team is aiming for a project completion date of 30 September 2011.

Chapter 3

Proposed Blind Signal Separation Approach

3.1 Introduction

The impact of performing the spatial dimensional processing of information signals via multiple antennas at the input and the output of a transceiver system on the improvement in information capacities is widely known. Specifically, with increasing signal-to-noise ratio (SNR), capacity gains can be achieved in the case of a multiple-input multiple output (MIMO) communication system compared to a single-input single-output (SISO) system, for a fixed overall transmit power by exploiting the spatial dimension [2, 3]. The performance requirement targets of several emerging beyond 3rd generation (B3G) and 4th generation (4G) wireless mobile communications standards include the need to provide siginificantly increased data-rates compared to their predecessors, particularly in the downlink [4]. Moreover, MIMO technology in combination with orthogonal frequency division multiplexing (OFDM) is the preferred candidate scheme due to the latter's low receiver complexity and high performance in time-dispersive channels.

A necessary condition for practical wireless transceivers operating over these standards to achieve the capacity gains offered by employing multiple antennas is the knowledge of channel state information (CSI) both at the receiver and the transmitter. The impact of imperfect channel state information on attained capacity is also widely investigated [5]. During the past two decades, several blind channel estimation techniques have been proposed which can be broadly categorized as statistical or deterministic methods depending on whether the statistical knowledge about the transmit antenna is exploited or not. For a detailed summary, see [6]. A common feature of several of these techniques proposed during the first decade is that their application is restricted to a point-to-point communications scenario with single input at the transmitter and possibly multiple outputs at the receiver *i.e.*, the channel is single-input/multiple-output (SIMO). While deterministic methods allow closed-form solutions, avoid local minima and offer high speed of convergence, they also suffer from channel length indeterminancies and require that the corresponding SIMO channel transfer function be irreducible [7, 8]. On the other hand, statistical methods are robust to channel length overdeterminancies and in the case of statistical maximum likelihood (ML)- based

approaches, no assumption is required on the knowledge of channel length [6]. However, these techniques require *a priori* knowledge of the probability density function (pdf) of the unknown input symbols, and the channel individually as well as jointly. These techniques are also optimal for large data sets and require proper initialization to avoid the possibility of attaining local minima.

Notation The notations used in this paper are fairly standard. Matrices and vectors are denoted by bold uppercase and bold lowerface letters. $(.)^{\mathrm{T}}$, $(.)^{\mathrm{H}}$ and $(.)^*$ represent transpose, Hermitian and conjugate operations respectively. $(.)^{1/2}$ represents the Hermitian square root of a matrix. $\otimes$ stands for Kronecker product of matrices. $\mathbf{I}_r$ denotes a $r \times r$ identity matrix. The vectorization operation, vec $([\mathbf{x}_1\ \mathbf{x}_2\ ...\ \mathbf{x}_K])$ equals $[\mathbf{x}_1^{\mathrm{T}}\ \mathbf{x}_2^{\mathrm{T}}\ ...\ \mathbf{x}_K^{\mathrm{T}}]^{\mathrm{T}}$. Moreover, when explicit itemize is omitted, $\mathbf{x}$ is understood to mean vec $(\mathbf{X})$. $\mathbf{z} \sim \mathcal{CN}(\mathbf{0}, \mathbf{R})$ indicates that the random vector $\mathbf{z}$ is drawn from a complex Gaussian distribution with $\mathbf{0}$ being the mean vector and $\mathbf{R}$, the correlation matrix. We also state here, certain well-known identities involving vectorization and Kronecker product operations which will be used in the following sections

($\mathbb{I}1$) vec $(\mathbf{A} \pm \mathbf{B}) =$ vec $(\mathbf{A}) \pm$ vec $(\mathbf{B})$

($\mathbb{I}2$) $(\mathbf{B}^T \otimes \mathbf{A})$vec $(\mathbf{X}) =$ vec $(\mathbf{AXB})$

($\mathbb{I}3$) $(\mathbf{A} \otimes \mathbf{B})(\mathbf{C} \otimes \mathbf{D}) = (\mathbf{AC} \otimes \mathbf{BD})$

($\mathbb{I}4$) $(\mathbf{A} \otimes \mathbf{C}) + (\mathbf{B} \otimes \mathbf{C}) = (\mathbf{A} + \mathbf{B}) \otimes \mathbf{C}$

3.2 MU-MIMO Wireless Channel Mixing Model

The MU-MIMO system model used in our analysis is a single-input multiple-antenna broadcast channel. We consider a J-channel FIR system excited by K transmit antennas with J and K being possibly unequal. A *quasi* time-invariant multipath channel is assumed which remains constant during the transmission of a set of consecutive symbols, hereafter referrred to as a *slot*, and changes its characteristics independently during the transmission of any other slot. The channel estimation is performed over each slot. Each symbol inside a slot is assumed to be the result of a known redundant precoder acting on an input transmit symbol vector drawn from an M-PSK or M-QAM constellation. The desired user receives signals not only from the intended transmitter but also from Q other interferers. The interferers are assumed to employ the same redundant precoder as the desired transmitter. Thus, the environment in which the desired transmitter operates is assumed to be interference-rich and the effect of the thermal noise is neglected. The overall system model is shown in Figure 3.1.

A matrix formulation of this system is as follows. Assuming that the downsampling factor at the input of the precoder for the kth transmit antenna to be M, we arrange the information data vector representing M-sized blocks as shown below:

$$\mathbf{d}_k(nM) \triangleq [d_k(nM + M - 1)\ ...\ d_k(nM)]^{\mathrm{T}} \tag{3.1}$$

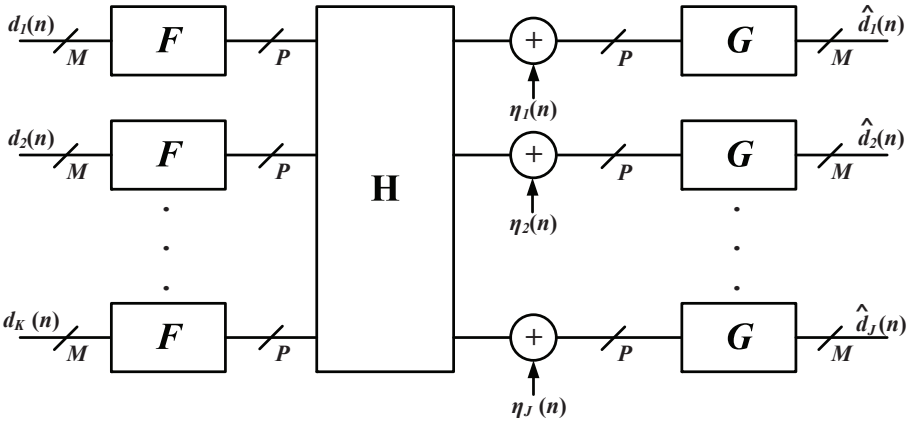

Figure 3.1: MU-MIMO transceiver model with N_t transmit and N_r receive antennas

where, $d_k(nM+m)$ represents the mth symbol in the nth block containing M symbols which is transmitted by the kth transmit antenna. An expression for the precoded symbol[1], $\mathbf{x}_k(nP)$ is now obtained as the product of a full-column precoder matrix,

$$\mathbf{F}^{(k)} \triangleq \begin{bmatrix} f_{M-1}^{(k)}(P-1) & f_{M-2}^{(k)}(P-1) & \dots & f_0^{(k)}(P-1) \\ f_{M-1}^{(k)}(P-2) & f_{M-2}^{(k)}(P-2) & \dots & f_0^{(k)}(P-2) \\ \vdots & \vdots & \ddots & \vdots \\ f_{M-1}^{(k)}(0) & f_{M-2}^{(k)}(0) & \dots & f_0^{(k)}(0) \end{bmatrix} \tag{3.2}$$

and $\mathbf{d}_k(nM)$ as:

$$\mathbf{x}_k(nP) = [x_k(nP+P-1) \ \dots \ x_k(nP)]^{\mathrm{T}} = \mathbf{F}^{(k)}\mathbf{d}_k(nM) \tag{3.3}$$

We assume that N precoded symbols constitute one slot and assign $n = 0$ in the sequel without loss of generality.

With $\dot{\mathbf{y}}_{jk} \triangleq [\dot{y}_{jk}((N-1)P+P-1) \dots \dot{y}_{jk}((N-1)P+L) \dots \dot{y}_{jk}(0.P+P-1) \dots \dot{y}_{jk}(0.P+L)]^{\mathrm{T}}$, we can define the interference-free output of the channel in terms of a Toeplitz matrix representing the channel between the kth transmit and jth receive antennas,

$$\mathcal{T}(\mathbf{H}_{jk}) \triangleq \begin{bmatrix} h_{jk}(0) & \dots & h_{jk}(L-1) & \dots & 0 \\ \vdots & \ddots & \ddots & \ddots & \vdots \\ 0 & \dots & h_{jk}(0) & \dots & h_{jk}(L-1) \end{bmatrix}$$

and the column vector representing the information symbols transmitted, $\mathbf{x}_k \triangleq \mathrm{vec}([\mathbf{x}_k((N-1)P) \ \mathbf{x}_k((N-2)P) \ \dots \ \mathbf{x}_k(0.P)])$, as:

$$\dot{\mathbf{y}}_{jk} = \mathbf{H}_{jk}\,\mathbf{x}_k \tag{3.4}$$

where, $\mathbf{H}_{jk} \triangleq (\mathbf{I}_N \otimes \mathcal{T}(\mathbf{H}_{jk}))$. In writing eq. (3.4), we assumed that the channel order between any transmit-receive pair in the system is L, such that $P = M + L$. Moreover, it

[1]We refer to each size-P block at the output of the transmit filterbank precoder as a "precoded symbol"

can be noticed from the definition of $\dot{\mathbf{y}}_{jk}$ that the first L elements of each received precoded symbol have been discarded to eliminate interference from the previous precoded symbol. An alternative representation for the interference-free output of the channel can be given as the product of a Hankel matrix containing the information symbols,

$$\mathcal{H}(\mathbf{x}_k) \triangleq \begin{bmatrix} x_k((N-1)P+P-1) & \dots & x_k((N-1)P+P-L) \\ \vdots & \ddots & \vdots \\ x_k(L) & \dots & x_k(0) \end{bmatrix}$$

and a column vector, $\mathbf{h}_{jk} \triangleq [h_{jk}(0) \ \dots \ h_{jk}(L-1)]^{\mathrm{T}}$ representing the channel as,

$$\ddot{\mathbf{y}}_{jk} = \mathcal{H}(\mathbf{x}_k)\, \mathbf{h}_{jk} \tag{3.5}$$

With $\dot{\mathbf{y}}_k \triangleq \mathrm{vec}\left([\dot{\mathbf{y}}_{1k} \dots \dot{\mathbf{y}}_{Jk}]\right)$, the composite interference-free signal from K transmit antennas received over J channels can be given based on eq.s (3.4) and (3.5), as follows:

$$\boldsymbol{\mu}_{\mathrm{y}} = \sum_{k=1}^{K} \dot{\mathbf{y}}_k = \sum_{k=1}^{K} [\mathbf{H}_{1k}^{\mathrm{T}} \ \dots \ \mathbf{H}_{Jk}^{\mathrm{T}}]^{\mathrm{T}}\, \mathbf{x}_k \tag{3.6}$$

$$\boldsymbol{\mu}_{\mathrm{y}} = \sum_{k=1}^{K} \ddot{\mathbf{y}}_k = \sum_{k=1}^{K} \mathrm{vec}\left(\mathcal{H}(\mathbf{x}_k)\, [\mathbf{h}_{1k} \ \dots \ \mathbf{h}_{Jk}]\right) = \sum_{k=1}^{K} (\mathbf{I}_J \otimes \mathcal{H}(\mathbf{x}_k))\, \mathbf{h}_k \tag{3.7}$$

We now develop the model for the interference vector using an alternative approach. The signal received from qth interferer is as follows:

$$\mathbf{W}^{(q)} \triangleq \sum_{l=0}^{L-1} \mathbf{X}_{(-l)}^{(q)} \underline{\mathbf{H}}_l^{(q)} \tag{3.8}$$

where, the discrete composite channel matrix for the lth lag, $\underline{\mathbf{H}}_l^{(q)}$, is defined such that $\left[\underline{\mathbf{H}}_l^{(q)}\right]_{n_t,n_r} = h_{n_t,n_r}^{(q)}(l)$ and

$$\mathbf{X}_0^{(q)} \triangleq \begin{bmatrix} \mathbf{x}_1^{(q)}((K-1)P) & \dots & \mathbf{x}_J^{(q)}((K-1)P) \\ \mathbf{x}_1^{(q)}((K-2)P) & \dots & \mathbf{x}_J^{(q)}((K-1)P) \\ \vdots & \ddots & \vdots \\ \mathbf{x}_1^{(q)}(0) & \dots & \mathbf{x}_J^{(q)}(0) \end{bmatrix}$$

with $\mathbf{x}_j^{(q)}(nP)$ defined as in eq. (3.41). Also,

$$\mathbf{X}_{(-l)}^{(q)} \triangleq \left[\begin{array}{c|c} \mathbf{X}_0^{(q)\mathrm{T}}(:, l+1:end) & \begin{array}{c} \mathbf{x}_1^{(q)}(-1)^{\mathrm{T}}(:, 1:l) \\ \vdots \\ \mathbf{x}_J^{(q)}(-1)^{\mathrm{T}}(:, 1:l) \end{array} \end{array}\right]^{\mathrm{T}}$$

where the MATLAB notation indicating the selection of columns applies to the transposed variables. Rewriting eq. (3.8) by utilizing the knowledge of the transmit precoder,

$$\mathbf{W}^{(q)} = \sum_{l=0}^{L-1} (\mathbf{I}_K \otimes \mathbf{F}_{(-l)}^{(k)}) \mathbf{D}_{(-l)}^{(q)} \underline{\mathbf{H}}_l^{(q)} \tag{3.9}$$

where, $\mathbf{D}_{(-l)}^{(q)}$ is defined similar to $\mathbf{X}_{(-l)}^{(q)}$ and $\mathbf{F}_{(-l)}^{(k)} = \left[\mathbf{F}^{(k)}(:, l+1:end)\ \mathbf{F}^{(k)}(:, 1:l)\right]$. The vectorization form of eq. (3.9) obtained by applying (𝕀1) and (𝕀2) is now,

$$\mathbf{w}^{(q)} = \sum_{l=0}^{L-1} (\underline{\mathbf{H}}_l^{(q)\mathrm{T}} \otimes \mathbf{I}_K \otimes \mathbf{F}_{(-l)}^{(k)})\, \mathbf{d}_{(-l)}^{(q)} \tag{3.10}$$

By assuming that the input to the transmit precoder of the qth interferer is a sequence of i.i.d standard normal complex random variables, the auto-correlation matrix of $\mathbf{w}^{(q)}$ by applying the vectorization identities, (𝕀3) and (𝕀4), is,

$$\mathbf{R}_{\mathbf{w}}^{(q)} = E\left[\mathbf{w}^{(q)}\, \mathbf{w}^{(q)\mathrm{H}}\right] = (\mathbf{R}_q \otimes \mathbf{I}_K \otimes \mathbf{R}_{\mathbf{F}}) \tag{3.11}$$

where $\mathbf{R}_{\mathbf{F}} \triangleq \mathbf{F}_{(-l)}^{(k)} \mathbf{F}_{(-l)}^{(j)\mathrm{H}} = \mathbf{F}^{(j)\mathrm{H}} \mathbf{F}^{(k)}$ irrespective of the value of l and is a known Hermitian matrix since $\mathbf{F}^{(k)}$ is a matrix of full column-rank M. Also, $\mathbf{R}_q \triangleq \sum_{l=0}^{L_q-1} \underline{\mathbf{H}}_l^{(q)\mathrm{T}} \underline{\mathbf{H}}_l^{(q)*}$. Thus, the auto-correlation matrix of the interference due to Q interferers is found by applying (𝕀4) as,

$$\mathbf{R}_{\mathbf{w}} = \sum_{q=1}^{Q} \mathbf{R}_{\mathbf{w}}^{(q)} = (\mathbf{R}_{\mathbf{S}} \otimes \mathbf{I}_K \otimes \mathbf{R}_{\mathbf{F}}) \tag{3.12}$$

where $\mathbf{R}_{\mathbf{S}} \triangleq \sum_{q=1}^{Q} \mathbf{R}_q$. It can be noticed that in eq. (3.12), $\mathbf{R}_{\mathbf{S}}$ represents its spatial auto-correlation across K receive antennas and $\mathbf{I}_K \otimes \mathbf{R}_{\mathbf{F}}$ represents the temporal auto-correlation of the interference across K P-sized blocks which is assumed to be time-invariant over K symbols. Due to the summations involved in deriving eq. (3.11) over the channel orders of each of the interferers, no assumptions are necessary regarding the number of the transmit antennas of each of the interferers and the channel orders as long as they are smaller than P. Similarly, due to the summations over the number of interferers in eq. (3.12), no assumptions are necessary regarding their number. On the other hand, the unknown matrix, $\mathbf{R}_{\mathbf{S}}$ is assumed to be Hermitian positive-definite with $(K(K+1)/2)$ unknown complex elements. We now have two equivalent versions for the likelihood function,

$$p(\mathbf{y}; \boldsymbol{\theta}) \sim \mathcal{CN}\left(\boldsymbol{\mu}_{\mathrm{y}}, \mathbf{R}_{\mathbf{w}}\right) \tag{3.13}$$

based on eq.s (3.6) and (3.7). Thus, $\boldsymbol{\mu}_{\mathrm{y}} = \sum_{j=1}^{J} (\mathbf{I}_K \otimes \mathcal{H}(\mathbf{x}_j))\, \mathbf{h}_j = \sum_{j=1}^{J} \mathbf{H}_j\, \mathbf{x}_j$, and $p(\mathbf{y}; \boldsymbol{\theta})$ is parameterized by the vector, $\boldsymbol{\theta} = [\mathbf{h}_1^{\mathrm{T}},\ \mathbf{x}_1^{\mathrm{T}},\ ...,\ \mathbf{h}_J^{\mathrm{T}},\ \mathbf{x}_J^{\mathrm{T}},\ \mathrm{diag}\,(\mathbf{R}_{\mathbf{S}})^{\mathrm{T}},\ \mathrm{vec}_l\,(\mathbf{R}_{\mathbf{S}})^{\mathrm{T}}]^{\mathrm{T}}$ where, $\dim(\boldsymbol{\theta}) = LJK + KPJ + (K(K+1)/2)$.

3.3 Fisher Information Matrix

We now derive the FIM for the MU-MIMO communication system model described in Section 3.2 and show that it is rank-deficient. In following theorem, the vectors, $\mathbf{h}_j$s and $\mathbf{x}_j$s from eq. (3.13) are treated as deterministic unknowns.

Theorem 1: Assuming that the likelihood funtion, $p(\mathbf{y}; \boldsymbol{\theta})$ described in eq. (3.13) satisfies the regularity condition, the complex FIM for the interference-limited MU-MIMO communication system model is given by the matrix,

$$\mathbf{I}_{\mathrm{c}}(\boldsymbol{\theta}) = \begin{bmatrix} \mathbf{I}_{\mathrm{c}}(\boldsymbol{\theta})_{1,1} & \mathbf{I}_{\mathrm{c}}(\boldsymbol{\theta})_{1,2} \\ \mathbf{I}_{\mathrm{c}}(\boldsymbol{\theta})_{2,1} & \mathbf{I}_{\mathrm{c}}(\boldsymbol{\theta})_{2,2} \end{bmatrix} \tag{3.14}$$

In eq. (3.14),

(i) $\mathbf{I}_{\mathrm{c}}(\boldsymbol{\theta})_{1,1} = \mathcal{Q}^{\mathrm{H}}\mathbf{R}_{\mathbf{w}}^{-1}\mathcal{Q} = \begin{bmatrix} \mathcal{Q}_1^{\mathrm{H}}\mathbf{R}_{\mathbf{w}}^{-1}\mathcal{Q}_1 & \dots & \mathcal{Q}_1^{\mathrm{H}}\mathbf{R}_{\mathbf{w}}^{-1}\mathcal{Q}_J \\ \vdots & \ddots & \vdots \\ \mathcal{Q}_J^{\mathrm{H}}\mathbf{R}_{\mathbf{w}}^{-1}\mathcal{Q}_1 & \dots & \mathcal{Q}_J^{\mathrm{H}}\mathbf{R}_{\mathbf{w}}^{-1}\mathcal{Q}_J \end{bmatrix}$
where, $\mathcal{Q} \triangleq [\mathcal{Q}_1 \ \dots \ \mathcal{Q}_J]$ such that, $\mathcal{Q}_j = [(\mathbf{I}_K \otimes \mathcal{H}(\mathbf{x}_j)) \ \ \mathbf{H}_j]$

(ii) $\mathbf{I}_{\mathrm{c}}(\boldsymbol{\theta})_{2,2} = \mathcal{R}^{\mathrm{H}}\mathcal{R}$
where, $\mathcal{R} = [(\mathbf{R}_{\mathbf{w}}^{-1/2} \otimes \mathbf{R}_{\mathbf{w}}^{-\mathrm{T}/2})\,\mathcal{A}(\mathbf{F}^{(k)})^{\mathrm{H}}\,\boldsymbol{L}_d \quad (\mathbf{R}_{\mathbf{w}}^{-1/2} \otimes \mathbf{R}_{\mathbf{w}}^{-\mathrm{T}/2})\,\mathcal{A}(\mathbf{F}^{(k)})^{\mathrm{H}}\,\boldsymbol{L}_u]$. Here, $\mathcal{A}(\mathbf{F}^{(k)})^{\mathrm{T}} \triangleq [\mathbf{I}_K \otimes \mathcal{K}_{KPK} \otimes \mathbf{I}_{KP}]\,[\mathbf{I}_{K^2} \otimes \mathrm{vec}(\mathbf{I}_K \otimes \mathbf{R}_{\mathbf{F}})]$ and $\boldsymbol{L}_d$, $\boldsymbol{L}_l$, and $\boldsymbol{L}_u$ are matrices formed from the commutation matrix, $\mathcal{K}_{K^2}$ such that, $\mathrm{vec}\,(\mathbf{R}_{\mathbf{S}}) = \boldsymbol{L}_d\,\mathrm{diag}\,(\mathbf{R}_{\mathbf{S}}) + \boldsymbol{L}_l\,\mathrm{vec}_l\,(\mathbf{R}_{\mathbf{S}}) + \boldsymbol{L}_u\,\mathrm{vec}_u\,(\mathbf{R}_{\mathbf{S}})$

(iii) $\mathbf{I}_{\mathrm{c}}(\boldsymbol{\theta})_{1,2} = \mathbf{I}_{\mathrm{c}}(\boldsymbol{\theta})_{2,1} = \mathbf{0}$

Proof. From [9], we know that the complex FIM is given by the equation,

$$\mathbf{I}_{\mathrm{c}}(\boldsymbol{\theta}) = E\left[\left(\frac{\partial \ln p(\mathbf{y};\boldsymbol{\theta})}{\partial\,\boldsymbol{\theta}^*}\right)\left(\frac{\partial \ln p(\mathbf{y};\boldsymbol{\theta})}{\partial\,\boldsymbol{\theta}^*}\right)^{\mathrm{H}}\right] \tag{3.15}$$

The log-likelihood function is given by the equation,

$$\ln p(\mathbf{y};\boldsymbol{\theta}) = -KPK\ln(\pi) \ - \ln\det(\mathbf{R}_{\mathbf{w}}) \ - (\mathbf{y}-\boldsymbol{\mu}_{\mathrm{y}})^{\mathrm{H}}\,\mathbf{R}_{\mathbf{w}}^{-1}\,(\mathbf{y}-\boldsymbol{\mu}_{\mathrm{y}}) \tag{3.16}$$

(i) $\underline{\mathbf{I}_{\mathrm{c}}(\boldsymbol{\theta})_{1,1}}$: The partial derivatives of the log-likelihood function shown in eq. (3.16) w.r.t $\mathbf{h}_j^*$ and $\mathbf{x}_j^*$ are as follows:

$$\frac{\partial \ln p(\mathbf{y};\boldsymbol{\theta})}{\partial \mathbf{h}_j^*} \ = \ (\mathbf{I}_K \otimes \mathcal{H}(\mathbf{x}_j))^{\mathrm{H}}\,\mathbf{R}_{\mathbf{w}}^{-1}\,(\mathbf{y} - \sum_{j=1}^{J}(\mathbf{I}_K \otimes \mathcal{H}(\mathbf{x}_j))\,\mathbf{h}_j) \tag{3.17}$$

$$\frac{\partial \ln p(\mathbf{y};\boldsymbol{\theta})}{\partial \mathbf{x}_j^*} \ = \ \mathbf{H}_j^{\mathrm{H}}\,\mathbf{R}_{\mathbf{w}}^{-1}\,(\mathbf{y} - \sum_{j=1}^{J}\mathbf{H}_j\,\mathbf{x}_j) \tag{3.18}$$

Substituting eq.s (3.17) and (3.18) in eq. (3.15), the associated FIM for the parameter vector $[\mathbf{h}_j^{\mathrm{T}},\ \mathbf{x}_j^{\mathrm{T}}]^{\mathrm{T}}$ is:

$$\mathcal{Q}_j^{\mathrm{H}}\mathbf{R}_{\mathbf{w}}^{-1}\mathcal{Q}_j = \begin{bmatrix} (\mathbf{I}_K \otimes \mathcal{H}(\mathbf{x}_j))^{\mathrm{H}}\,\mathbf{R}_{\mathbf{w}}^{-1}\,(\mathbf{I}_K \otimes \mathcal{H}(\mathbf{x}_j)) & (\mathbf{I}_K \otimes \mathcal{H}(\mathbf{x}_j))^{\mathrm{H}}\,\mathbf{R}_{\mathbf{w}}^{-1}\,\mathbf{H}_j \\ \mathbf{H}_j^{\mathrm{H}}\,\mathbf{R}_{\mathbf{w}}^{-1}\,(\mathbf{I}_K \otimes \mathcal{H}(\mathbf{x}_j)) & \mathbf{H}_j^{\mathrm{H}}\,\mathbf{R}_{\mathbf{w}}^{-1}\,\mathbf{H}_j \end{bmatrix} \tag{3.19}$$

Therefore, by extension, the FIM associated with $[\mathbf{h}_1^{\mathrm{T}},\ \mathbf{x}_1^{\mathrm{T}},\ \dots,\ \mathbf{h}_J^{\mathrm{T}},\ \mathbf{x}_J^{\mathrm{T}},]^{\mathrm{T}}$,

$$\mathbf{I}_{\mathrm{c}}(\boldsymbol{\theta})_{1,1} = \mathcal{Q}^{\mathrm{H}}\mathbf{R}_{\mathbf{w}}^{-1}\mathcal{Q} \tag{3.20}$$

where, $\mathcal{Q} \triangleq [\mathcal{Q}_1 \ \dots \ \mathcal{Q}_J]$ such that, $\mathcal{Q}_j = [(\mathbf{I}_K \otimes \mathcal{H}(\mathbf{x}_j)) \ \ \mathbf{H}_j]$.
(ii) $\underline{\mathbf{I}_{\mathrm{c}}(\boldsymbol{\theta})_{2,2}}$: In order to evaluate the partial derivatives involved in identifying the FIM of the likelihood function shown in eq. (3.13) w.r.t $[\mathrm{diag}\,(\mathbf{R}_{\mathbf{S}})^{\mathrm{T}},\ \mathrm{vec}_l\,(\mathbf{R}_{\mathbf{S}})^{\mathrm{T}}]^{\mathrm{T}}$, we apply the chain rule for finding partial derivatives of a complex-valued patterned matrix as outlined in [10, Theorem 1]. The statement of the theorem and a brief discussion is provided here for reference. For a detailed introduction to the framework on determining the derivatives of a general complex-valued matrix function using complex differentials, see [11].

Theorem (Chain Rule [10])**:** Let $(S_0, S_1, S_2) \subseteq \mathbb{R}^{K\times L} \times \mathbb{C}^{N\times Q} \times \mathbb{C}^{N\times Q}$, and let $\boldsymbol{F} : S_0 \times S_1 \times S_2 \to \mathbb{C}^{M\times P}$ be differentiable w.r.t its first, second and third argument at an interior point $(\boldsymbol{X}, \boldsymbol{Z}, \boldsymbol{Z}^*)$ in the set $S_0 \times S_1 \times S_2$. Let $T_0 \times T_1 \subseteq \mathbb{C}^{M\times P} \times \mathbb{C}^{M\times P}$ be such that $(\boldsymbol{F}(\boldsymbol{X}, \boldsymbol{Z}, \boldsymbol{Z}^*, \boldsymbol{F}^*(\boldsymbol{X}, \boldsymbol{Z}, \boldsymbol{Z}^*)) \in T_0 \times T_1$ for all $(\boldsymbol{X}, \boldsymbol{Z}, \boldsymbol{Z}^*) \in S_0 \times S_1 \times S_2$. Assume that $\boldsymbol{G} : T_0 \times T_1 \to \mathbb{C}^{R\times S}$ is differentiable at an interior point $(\boldsymbol{F}(\boldsymbol{X}, \boldsymbol{Z}, \boldsymbol{Z}^*, \boldsymbol{F}^*(\boldsymbol{X}, \boldsymbol{Z}, \boldsymbol{Z}^*) \in T_0 \times T_1$. Define the composite function $\boldsymbol{H} : S_0 \times S_1 \times S_2 \to \mathbb{C}^{R\times S}$ by $\boldsymbol{H}(\boldsymbol{X}, \boldsymbol{Z}, \boldsymbol{Z}^*)) \triangleq \boldsymbol{G}(\boldsymbol{F}(\boldsymbol{X}, \boldsymbol{Z}, \boldsymbol{Z}^*, \boldsymbol{F}^*(\boldsymbol{X}, \boldsymbol{Z}, \boldsymbol{Z}^*))$. The derivatives $\mathcal{D}_{\boldsymbol{X}}\boldsymbol{H}$, $\mathcal{D}_{\boldsymbol{Z}}\boldsymbol{H}$ and $\mathcal{D}_{\boldsymbol{Z}^*}\boldsymbol{H}$ are:

$$\mathcal{D}_{\boldsymbol{X}}\boldsymbol{H} = (\mathcal{D}_{\boldsymbol{F}}\boldsymbol{G})\,\mathcal{D}_{\boldsymbol{X}}\boldsymbol{F} \;+\; (\mathcal{D}_{\boldsymbol{F}^*}\boldsymbol{G})\,\mathcal{D}_{\boldsymbol{X}}\boldsymbol{F}^* \tag{3.21}$$

$$\mathcal{D}_{\boldsymbol{Z}}\boldsymbol{H} = (\mathcal{D}_{\boldsymbol{F}}\boldsymbol{G})\,\mathcal{D}_{\boldsymbol{Z}}\boldsymbol{F} \;+\; (\mathcal{D}_{\boldsymbol{F}^*}\boldsymbol{G})\,\mathcal{D}_{\boldsymbol{Z}}\boldsymbol{F}^* \tag{3.22}$$

$$\mathcal{D}_{\boldsymbol{Z}^*}\boldsymbol{H} = (\mathcal{D}_{\boldsymbol{F}}\boldsymbol{G})\,\mathcal{D}_{\boldsymbol{Z}^*}\boldsymbol{F} \;+\; (\mathcal{D}_{\boldsymbol{F}^*}\boldsymbol{G})\,\mathcal{D}_{\boldsymbol{Z}^*}\boldsymbol{F}^* \tag{3.23}$$

Following the notational convention of [10], the set of patterned matrices is denoted as, $\mathcal{W} \subseteq \mathbb{C}^{M\times P}$ and a particular patterned matrix as, $\boldsymbol{W} \in \mathcal{W}$, $\boldsymbol{W}$ is parameterized by the matrizes, $\boldsymbol{X}$ and $\boldsymbol{Z}$ through the relation, $\boldsymbol{W} = \boldsymbol{F}(\boldsymbol{X}, \boldsymbol{Z}, \boldsymbol{Z}^*)$, where $\boldsymbol{F}$ is referred to as *pattern producing function*. In order to apply the chain rule, the matrix functions $\boldsymbol{F}$ and $\boldsymbol{G}$ must be differentiable which is possible when these functions do not contain patterns. Therefore, we let the domain of the matrix function $\boldsymbol{G}$, to be the elements that belong to the larger set of unpatterned matrices, $\tilde{\mathcal{W}}$ such that when $\boldsymbol{G}(\tilde{\boldsymbol{W}}, \tilde{\boldsymbol{W}}^*)$ is restricted to the patterned matrices $\boldsymbol{W}$ and $\boldsymbol{W}^*$, we obtain the function whose derivative we want to find. In other words,

$$\begin{aligned}\boldsymbol{G}(\boldsymbol{W}, \boldsymbol{W}^*) &= \boldsymbol{G}(\tilde{\boldsymbol{W}}, \tilde{\boldsymbol{W}}^*)|_{\tilde{\boldsymbol{W}}=\boldsymbol{W}=\boldsymbol{F}(\boldsymbol{X},\boldsymbol{Z},\boldsymbol{Z}^*)} \\ &= \boldsymbol{G}(\boldsymbol{F}(\boldsymbol{X}, \boldsymbol{Z}, \boldsymbol{Z}^*, \boldsymbol{F}^*(\boldsymbol{X}, \boldsymbol{Z}, \boldsymbol{Z}^*)) \\ &\triangleq \boldsymbol{H}(\boldsymbol{X}, \boldsymbol{Z}, \boldsymbol{Z}^*))\end{aligned} \tag{3.24}$$

Hence, the derivative of $\boldsymbol{H}(\boldsymbol{X}, \boldsymbol{Z}, \boldsymbol{Z}^*))$ w.r.t $\boldsymbol{X}$, $\boldsymbol{Z}$ and $\boldsymbol{Z}^*$ can be written using the chain rule shown in eq.s (3.21), (3.22) and (3.23) as:

$$\begin{aligned}&\mathcal{D}_{\boldsymbol{X}}\boldsymbol{H}(\boldsymbol{X}, \boldsymbol{Z}, \boldsymbol{Z}^*)) \\ =\;& (\mathcal{D}_{\boldsymbol{F}}\boldsymbol{G}(\tilde{\boldsymbol{W}}, \tilde{\boldsymbol{W}}^*)|_{\tilde{\boldsymbol{W}}=\boldsymbol{W}=\boldsymbol{F}(\boldsymbol{X},\boldsymbol{Z},\boldsymbol{Z}^*)})\,\mathcal{D}_{\boldsymbol{X}}\boldsymbol{F}(\boldsymbol{X}, \boldsymbol{Z}, \boldsymbol{Z}^*) \\ +\;& (\mathcal{D}_{\boldsymbol{F}^*}\boldsymbol{G}(\tilde{\boldsymbol{W}}, \tilde{\boldsymbol{W}}^*)|_{\tilde{\boldsymbol{W}}=\boldsymbol{W}=\boldsymbol{F}(\boldsymbol{X},\boldsymbol{Z},\boldsymbol{Z}^*)})\,\mathcal{D}_{\boldsymbol{X}}\boldsymbol{F}^*(\boldsymbol{X}, \boldsymbol{Z}, \boldsymbol{Z}^*) \\ &\mathcal{D}_{\boldsymbol{Z}}\boldsymbol{H}(\boldsymbol{X}, \boldsymbol{Z}, \boldsymbol{Z}^*))\end{aligned} \tag{3.25}$$

$$\begin{aligned}=\;& (\mathcal{D}_{\boldsymbol{F}}\boldsymbol{G}(\tilde{\boldsymbol{W}}, \tilde{\boldsymbol{W}}^*)|_{\tilde{\boldsymbol{W}}=\boldsymbol{W}=\boldsymbol{F}(\boldsymbol{X},\boldsymbol{Z},\boldsymbol{Z}^*)})\,\mathcal{D}_{\boldsymbol{Z}}\boldsymbol{F}(\boldsymbol{X}, \boldsymbol{Z}, \boldsymbol{Z}^*) \\ +\;& (\mathcal{D}_{\boldsymbol{F}^*}\boldsymbol{G}(\tilde{\boldsymbol{W}}, \tilde{\boldsymbol{W}}^*)|_{\tilde{\boldsymbol{W}}=\boldsymbol{W}=\boldsymbol{F}(\boldsymbol{X},\boldsymbol{Z},\boldsymbol{Z}^*)})\,\mathcal{D}_{\boldsymbol{Z}}\boldsymbol{F}^*(\boldsymbol{X}, \boldsymbol{Z}, \boldsymbol{Z}^*) \\ &\mathcal{D}_{\boldsymbol{Z}^*}\boldsymbol{H}(\boldsymbol{X}, \boldsymbol{Z}, \boldsymbol{Z}^*))\end{aligned} \tag{3.26}$$

$$\begin{aligned}=\;& (\mathcal{D}_{\boldsymbol{F}}\boldsymbol{G}(\tilde{\boldsymbol{W}}, \tilde{\boldsymbol{W}}^*)|_{\tilde{\boldsymbol{W}}=\boldsymbol{W}=\boldsymbol{F}(\boldsymbol{X},\boldsymbol{Z},\boldsymbol{Z}^*)})\,\mathcal{D}_{\boldsymbol{Z}^*}\boldsymbol{F}(\boldsymbol{X}, \boldsymbol{Z}, \boldsymbol{Z}^*) \\ +\;& (\mathcal{D}_{\boldsymbol{F}^*}\boldsymbol{G}(\tilde{\boldsymbol{W}}, \tilde{\boldsymbol{W}}^*)|_{\tilde{\boldsymbol{W}}=\boldsymbol{W}=\boldsymbol{F}(\boldsymbol{X},\boldsymbol{Z},\boldsymbol{Z}^*)})\,\mathcal{D}_{\boldsymbol{Z}^*}\boldsymbol{F}^*(\boldsymbol{X}, \boldsymbol{Z}, \boldsymbol{Z}^*)\end{aligned} \tag{3.27}$$

It should be noted that, the definition of the partial derivative adopted by Hjørungnes *et al* for the case of a scalar function w.r.t a column vector, results in a row vector [11, Table III]. For the problem under consideration, we consider this definition to lead to transposed derivative. Therefore, we perform a transpose operation of the results obtained based on eq.s (3.25), (3.26) and (3.27) in order to obtain the FIM with proper dimensions.

Evaluating the partial derivatives of the two terms in eq. (3.16) that depend on diag $(\mathbf{R_S})$ separately, we first have,

$$\begin{aligned}\frac{\partial \ln\det(\mathbf{R_w})}{\partial\,\mathrm{diag}\,(\mathbf{R_S})} &= \frac{\partial \ln\det(\mathbf{R_w})}{\partial\,\mathbf{R_w}} \times \frac{\partial\,\mathbf{R_w}}{\partial\,\mathrm{diag}\,(\mathbf{R_S})} \\ &= [\,(\,\mathcal{D}_{\mathbf{R_w}} \ln\det(\mathbf{R_w}))\,\mathcal{D}_{\mathbf{R_S}}\mathbf{R_w}]^{\mathrm{T}} \\ &= [\,\mathrm{vec}^{\mathrm{T}}(\mathbf{R_w}^{-\mathrm{T}})\,\mathcal{A}(\mathbf{F}^{(k)})^{\mathrm{T}}\,d(\mathrm{vec}(\mathbf{R_S})\,)]^{\mathrm{T}} \\ &= \boldsymbol{L}_d^{\mathrm{T}}\,\mathcal{A}(\mathbf{F}^{(k)})\,\mathrm{vec}\,(\mathbf{R_w}^{-\mathrm{T}}) \end{aligned} \tag{3.28}$$

Here, $\mathcal{A}(\mathbf{F}^{(k)})^{\mathrm{T}} = [\mathbf{I}_K \otimes \mathcal{K}_{KPK} \otimes \mathbf{I}_{KP}]\,[\mathbf{I}_{K^2} \otimes \mathrm{vec}(\mathbf{I}_K \otimes \mathbf{R_F})]$ in the third equality and results due to [12, Theorem 3.10] whereas $\boldsymbol{L}_d$ in the fourth equality is an $K^2 \times K$ matrix that results from selecting the appropriate columns of the corresponding commutation matrix, $\mathcal{K}_{K^2}$ (see eq. (27) of [10] for an example). Similarly, we obtain,

$$\frac{\partial\,(\mathbf{y}-\boldsymbol{\mu}_{\mathrm{y}})^{\mathrm{H}}\,\mathbf{R_w}^{-1}\,(\mathbf{y}-\boldsymbol{\mu}_{\mathrm{y}})}{\partial\,\mathrm{diag}\,(\mathbf{R_S})} \tag{3.29}$$

$$= -\boldsymbol{L}_d^{\mathrm{T}}\,\mathcal{A}(\mathbf{F}^{(k)})\,\mathrm{vec}\,(\mathbf{R_w}^{-\mathrm{T}}\,(\mathbf{y}-\boldsymbol{\mu}_{\mathrm{y}})^{*}\,(\mathbf{y}-\boldsymbol{\mu}_{\mathrm{y}})^{\mathrm{T}}\,\mathbf{R_w}^{-\mathrm{T}})$$

$$= -\boldsymbol{L}_d^{\mathrm{T}}\,\mathcal{A}(\mathbf{F}^{(k)})\,[(\,\mathbf{R_w}^{-1/2} \otimes \mathbf{R_w}^{-\mathrm{T}/2}\,)\,(\,\underline{y} \otimes \underline{y}^{*}\,)] \tag{3.30}$$

where, $\underline{y} \triangleq \mathbf{R_w}^{-1/2}\,(\mathbf{y}-\boldsymbol{\mu}_{\mathrm{y}})$. The FIM associated with the parameter vector diag $(\mathbf{R_S})$ is now given by the expression,

$$E\left[\left(\frac{\partial \ln p(\mathbf{y};\boldsymbol{\theta})}{\partial\,\mathrm{diag}\,(\mathbf{R_S})}\right)\left(\frac{\partial \ln p(\mathbf{y};\boldsymbol{\theta})}{\partial\,\mathrm{diag}\,(\mathbf{R_S})}\right)^{\mathrm{H}}\right]$$

$$= \boldsymbol{L}_d^{\mathrm{T}}\,\mathcal{A}(\mathbf{F}^{(k)})\,[\,(\,\mathbf{R_w}^{-1/2} \otimes \mathbf{R_w}^{-\mathrm{T}/2}\,) \tag{3.31}$$

$$\times\quad E\,[(\,\underline{y} \otimes \underline{y}^{*}\,)\,(\,\underline{y}^{\mathrm{H}} \otimes \underline{y}^{\mathrm{T}}\,)]\,(\,\mathbf{R_w}^{-1/2} \otimes \mathbf{R_w}^{-\mathrm{T}/2}\,)$$

$$-\mathrm{vec}\,(\mathbf{R_w}^{-\mathrm{T}})\,\mathrm{vec}^{\mathrm{H}}\,(\mathbf{R_w}^{-\mathrm{T}})\,]\,\mathcal{A}(\mathbf{F}^{(k)})^{\mathrm{H}}\,\boldsymbol{L}_d$$

$$= \boldsymbol{L}_d^{\mathrm{T}}\,\mathcal{A}(\mathbf{F}^{(k)})\,(\,\mathbf{R_w}^{-1/2} \otimes \mathbf{R_w}^{-\mathrm{T}/2}\,) \tag{3.32}$$

$$\times\quad E\,[(\,\underline{y} \otimes \underline{y}^{*}\,)\,(\,\underline{y}^{\mathrm{H}} \otimes \underline{y}^{\mathrm{T}}\,) - \mathrm{vec}\,(\mathbf{I}_{KPK})\,\mathrm{vec}^{\mathrm{H}}\,(\mathbf{I}_{KPK})\,]$$

$$(\,\mathbf{R_w}^{-1/2} \otimes \mathbf{R_w}^{-\mathrm{T}/2}\,)\,\mathcal{A}(\mathbf{F}^{(k)})^{\mathrm{H}}\,\boldsymbol{L}_d$$

$$= \boldsymbol{L}_d^{\mathrm{T}}\,\mathcal{A}(\mathbf{F}^{(k)})\,(\,\mathbf{R_w}^{-1} \otimes \mathbf{R_w}^{-\mathrm{T}}\,)\,\mathcal{A}(\mathbf{F}^{(k)})^{\mathrm{H}}\,\boldsymbol{L}_d \tag{3.33}$$

Here, the third equality is a result of generalizing [13, Theorem 4.1]. Using a similar approach, we can show that,

$$E\left[\left(\frac{\partial \ln p(\mathbf{y};\boldsymbol{\theta})}{\partial\,\mathrm{vec}_l^{*}\,(\mathbf{R_S})}\right)\left(\frac{\partial \ln p(\mathbf{y};\boldsymbol{\theta})}{\partial\,\mathrm{vec}_l^{*}\,(\mathbf{R_S})}\right)^{\mathrm{H}}\right]$$

$$= \boldsymbol{L}_u^{\mathrm{T}}\,\mathcal{A}(\mathbf{F}^{(k)})\,(\,\mathbf{R_w}^{-1} \otimes \mathbf{R_w}^{-\mathrm{T}}\,)\,\mathcal{A}(\mathbf{F}^{(k)})^{\mathrm{H}}\,\boldsymbol{L}_u \tag{3.34}$$

where, $\boldsymbol{L}_u$ is of dimensions $K^2 \times K(K-1)/2$, and as before, it is formed from selecting the appropriate columns of the corresponding commutation matrix, $\mathcal{K}_{K^2}$. Hence, the FIM associated with the vector, $[\mathrm{diag}\,(\mathbf{R_S})^{\mathrm{T}},\ \mathrm{vec}_l\,(\mathbf{R_S})^{\mathrm{T}}]^{\mathrm{T}}$ is,

$$\mathbf{I}_{\mathrm{c}}(\boldsymbol{\theta})_{2,2} = \mathcal{R}^{\mathrm{H}}\mathcal{R} \tag{3.35}$$

where, $\mathcal{R} = [(\mathbf{R}_{\mathbf{w}}^{-1/2} \otimes \mathbf{R}_{\mathbf{w}}^{-\mathrm{T}/2})\,\mathcal{A}(\mathbf{F}^{(k)})^{\mathrm{H}}\,\boldsymbol{L}_d \quad (\mathbf{R}_{\mathbf{w}}^{-1/2} \otimes \mathbf{R}_{\mathbf{w}}^{-\mathrm{T}/2})\,\mathcal{A}(\mathbf{F}^{(k)})^{\mathrm{H}}\,\boldsymbol{L}_u]$.
(iii) $\underline{\mathbf{I}_{\mathrm{c}}(\boldsymbol{\theta})_{1,2} \text{ and } \mathbf{I}_{\mathrm{c}}(\boldsymbol{\theta})_{2,1}}$: In order to evaluate the FIM $\mathbf{I}_{\mathrm{c}}(\boldsymbol{\theta})_{2,1}$, we first observe that,

$$\begin{aligned} & E\left[\left(\frac{\partial \ln p(\mathbf{y};\boldsymbol{\theta})}{\partial\, \mathrm{diag}\,(\mathbf{R_S})}\right)\left(\frac{\partial \ln p(\mathbf{y};\boldsymbol{\theta})}{\partial\, \mathbf{h}_j^*}\right)^{\mathrm{H}}\right] \\ = \;& \boldsymbol{L}_d^{\mathrm{T}}\,\mathcal{A}(\mathbf{F}^{(k)})\,(\mathbf{R}_{\mathbf{w}}^{-1/2} \otimes \mathbf{R}_{\mathbf{w}}^{-\mathrm{T}/2})\,E\left[(\underline{y} \otimes \underline{y}^*)\,\underline{y}^{\mathrm{H}}\right]\mathbf{R}_{\mathbf{w}}^{-1/2}(\mathbf{I}_K \otimes \mathcal{H}(\mathbf{x}_j)) \\ = \;& \mathbf{0} \end{aligned} \tag{3.36}$$

since all third order mixed moments of a complex Gaussian random variable are equal to zero. We can similarly show that, $E\left[\left(\frac{\partial \ln p(\mathbf{y};\theta)}{\partial\, \mathrm{diag}\,(\mathbf{R_S})}\right)\left(\frac{\partial \ln p(\mathbf{y};\theta)}{\partial\, \mathbf{x}_j^*}\right)^{\mathrm{H}}\right]$, $E\left[\left(\frac{\partial \ln p(\mathbf{y};\theta)}{\partial\, \mathrm{vec}_l^*\,(\mathbf{R_S})}\right)\left(\frac{\partial \ln p(\mathbf{y};\theta)}{\partial\, \mathbf{h}_j^*}\right)^{\mathrm{H}}\right]$ and $E\left[\left(\frac{\partial \ln p(\mathbf{y};\theta)}{\partial\, \mathrm{vec}_l^*\,(\mathbf{R_S})}\right)\left(\frac{\partial \ln p(\mathbf{y};\theta)}{\partial\, \mathbf{x}_j^*}\right)^{\mathrm{H}}\right]$ are all equal to $\mathbf{0}$. Hence, by extension, $\mathbf{I}_{\mathrm{c}}(\boldsymbol{\theta})_{2,1}$ and $\mathbf{I}_{\mathrm{c}}(\boldsymbol{\theta})_{1,2} = \mathbf{I}_{\mathrm{c}}(\boldsymbol{\theta})_{2,1}^{\mathrm{H}}$ equal $\mathbf{0}$. □

3.4 Bayesian FIM

Under the following assumptions:

(A1) The filterbank output vector at the transmitter that corresponds to the information data $\mathbf{x}_d$ is an i.i.d sequence such that $\mathbf{x}_d \sim \mathcal{CN}(\mathbf{0}, \sigma_d^2)$. The power of pilot symbols over N_t packets is, $\sigma_\Gamma^2 = (1/n_\Gamma)\sum_{i=1}^{n_\gamma} |\mathbf{d}_\Gamma|^2$ where $n_\Gamma = \sum_{j=1}^{N_t} \gamma_j$ and $\mathbf{d}_\Gamma$ are the pilot symbols in the data vector, $\mathbf{d}$

(A2) The distribution over the MIMO channel vector, $\mathbf{h}$, is $p_h(.)$ and the interference vector, $\mathbf{w} \sim \mathcal{CN}(\mathbf{0}, \mathbf{R}_{\mathbf{w}})$

(A3) The vectors, $\mathbf{x}$, $\mathbf{h}$, and $\mathbf{w}$ and jointly independent

a Bayesian FIM can be written based on Theorem 1 as follows:

Corollary 1: Assuming that the likelihood funtion, $p(\mathbf{y};\boldsymbol{\theta})$ described in eq. (3.13) satisfies the regularity condition, the complex FIM for the parameter vector, $\boldsymbol{\theta} = [\mathbf{h}_1^{\mathrm{T}}, \mathbf{x}_1^{\mathrm{T}}, ..., \mathbf{h}_J^{\mathrm{T}}, \mathbf{x}_J^{\mathrm{T}}]^{\mathrm{T}}$, in an interference-limited MU-MIMO communication system model is given by the matrix,

$$\mathbf{I}_{\mathrm{c}}^B(\boldsymbol{\theta})_{1,1} = diag\,\left([\tilde{\mathcal{Q}}_1, \ldots \tilde{\mathcal{Q}}_J]\right) \tag{3.37}$$

where,

$$\begin{aligned} \tilde{\mathcal{Q}}_j \;\triangleq\; & \begin{bmatrix} E\{(\mathbf{I}_K \otimes \mathcal{H}(\mathbf{x}_j))^{\mathrm{H}}\,\mathbf{R}_{\mathbf{w}}^{-1}\,(\mathbf{I}_K \otimes \mathcal{H}(\mathbf{x}_j))\} & \mathbf{0} \\ \mathbf{0} & E\{\mathbf{H}_j^{\mathrm{H}}\,\mathbf{R}_{\mathbf{w}}^{-1}\,\mathbf{H}_j\} \end{bmatrix} \\ + \;& \begin{bmatrix} E\left\{\left|\frac{\partial \ln p_h(h)}{\partial h^*}\right|^2\right\} & \mathbf{0} \\ \mathbf{0} & E\left\{\left|\frac{\partial \ln p_x(x)}{\partial x^*}\right|^2\right\} \end{bmatrix} \end{aligned} \tag{3.38}$$

3.5 Future Work

3.5.1 Closed-Form Expression for the Co-channel Interference

Our future work also involves obtaining an alternate closed-form expression for the co-channel interference suffered by the desired receiver. An accurate modeling of this disturbance is expected to be vital in the interest of the proper design of training symbols. The itemize is as follows:

An equation for $\mathbf{w}$, in terms of data vector, $\mathbf{x}^{(q)}$ and the block Toeplitz composite channel matrix, $\mathcal{T}(\mathbf{H}^{(q)})$ can now be given as follows:

$$\mathbf{w} = \mathcal{T}(\mathbf{H}^{(q)})\ \mathbf{x}^{(q)} \tag{3.39}$$

The matrix describing the MIMO channel is given by the expression,

$$\mathcal{T}(\mathbf{H}^{(q)}) \triangleq \begin{pmatrix} \mathbf{H}_{\mathrm{L}-1} & \dots & \mathbf{H}_0 & \mathbf{0} & \dots & \mathbf{0} \\ \mathbf{0} & \mathbf{H}_{\mathrm{L}-1} & \dots & \mathbf{H}_0 & \dots & \mathbf{0} \\ \vdots & \ddots & \ddots & & \ddots & \vdots \\ \mathbf{0} & \dots & \mathbf{0} & \mathbf{H}_{\mathrm{L}-1} & \dots & \mathbf{H}_0 \end{pmatrix} \tag{3.40}$$

and

$$\mathbf{x}(nP+p) \triangleq [x_1(nP+p)\ \ x_2(nP+p)\ \ \dots\ \ x_{N_t}(nP+p)]^{\mathrm{T}} \tag{3.41}$$

$$\mathbf{x}_n \triangleq vec\left([\mathbf{x}(nP)\ \ \mathbf{x}(nP+1)\ \ \dots\ \ \mathbf{x}(nP+P-1)]\right) \tag{3.42}$$

$$\mathbf{x} \triangleq vec\left([\mathbf{x}_n\ \ \mathbf{x}_{n-1}\ \ \dots\ \ \mathbf{x}_{n-K+1}]\right) \tag{3.43}$$

In any practical MU-MIMO scenario, the channel matrix, $\mathcal{T}(\mathbf{H})$, does not consist of elements which are statistically independent, as is sometimes assumed. This assumption is invalid due to several factors such as transmit beamforming perfomed by the receiver, the close physical proximity of the receive antennas particularly in the case of mobile stations (MS), the delay profile of the channels etc. Therefore, the correlated MIMO channel model from [14] is applied in this work. Thus, the channel matrix for the lth lag is $\mathbf{H}_l = \mathbf{R}_{r,l}^{1/2}\mathbf{H}_{w,l}(\mathbf{R}_{t,l}^{1/2})^{\mathrm{T}}$ where the matrices $\mathbf{R}_{r,l}^{1/2}$ and $\mathbf{R}_{t,l}^{1/2}$ model the correlation between the receive and transmit antennas respectively. As a result, $\mathbf{h}_l = vec\,(\mathbf{H}_l) = (\mathbf{R}_{t,l}^{1/2} \otimes \mathbf{R}_{r,l}^{1/2})\mathbf{h}_{w,l}$ which is obtained by applying identity, ($\mathbb{I}$1). Matrix $\mathbf{H}_{w,l}$ consists of elements which are independent and identically distributed (i.i.d) zero-mean circular-symmetric complex Gaussian random variables with unit variance. We now have $\mathbf{h} = vec\,([\mathbf{h}_{L-1}\ \ \mathbf{h}_{L-2}\ \ \dots\ \ \mathbf{h}_0]) = \mathbf{C}_{rt}^{1/2}\mathbf{h}_w$ where

$$\mathbf{C}_{rt}^{1/2} \triangleq (\mathbf{R}_{r,L-1}^{1/2} \otimes \mathbf{R}_{t,L-1}^{1/2}) \oplus (\mathbf{R}_{r,L-2}^{1/2} \otimes \mathbf{R}_{t,L-2}^{1/2}) \oplus\ \ \dots\ \ \oplus (\mathbf{R}_{r,0}^{1/2} \otimes \mathbf{R}_{t,0}^{1/2}) \tag{3.44}$$

with $\mathbf{h}_w = vec\,([\mathbf{h}_{w,L-1}\ \ \mathbf{h}_{w,L-2}\ \ \dots\ \ \mathbf{h}_{w,0}])$.

Lemma 1: The covariance matrix of interference, $\boldsymbol{\Xi}$ is,

$$\mathbf{R}_{\boldsymbol{\Xi}} = \sum_{q=1}^{Q} \mathbf{R}_{\hat{\mathbf{y}}}^{(q)} \otimes \mathbf{R}_r = \mathbf{R}_{\hat{\mathbf{y}}}^{(Q)} \otimes \mathbf{R}_r \tag{3.45}$$

where

$$\mathbf{R}_{\hat{\mathbf{y}}}^{(Q)} \triangleq \sum_{q=1}^{Q} \mathbf{R}_{\hat{\mathbf{y}}}^{(q)} \tag{3.46}$$

with

$$\mathbf{R}_{\hat{\mathbf{y}}}^{(q)} \triangleq \begin{pmatrix} \sum_{j=1}^{N_t} R_{j,j}^{(q),n}(0) & \dots & \sum_{j=1}^{N_t} R_{j,j}^{(q),n-K+1}(P-L) \\ \vdots & \ddots & \vdots \\ \sum_{j=1}^{N_t} R_{j,j}^{(q),n}(L-1) & \dots & \sum_{j=1}^{N_t} R_{j,j}^{(q),n-K+1}(P-1) \end{pmatrix} \tag{3.47}$$

and

$$\mathbf{R}_r^{1/2} \triangleq [\mathbf{R}_{r,L-1}^{1/2} \ \mathbf{R}_{r,L-2}^{1/2} \ \dots \ \mathbf{R}_{r,0}^{1/2}] \tag{3.48}$$

$$\mathbf{R}_r \triangleq \mathbf{R}_r^{1/2} \times (\mathbf{R}_r^{1/2})^{\mathrm{H}} \tag{3.49}$$

Proof. Let the signal received by the desired user from the qth interferer be $\mathbf{\Xi}^{(q)} = \mathcal{H}(\mathbf{x}^{(q)})\ \mathbf{h}^{(q)}$ where $\mathcal{H}(\mathbf{x}^{(q)})$ is defined as in eq. (3.5). By applying identity, ($\mathbb{I}$1), we now have,

$$\mathbf{\Xi}^{(q)} = vec\,(\Xi^{(q)}) \tag{3.50}$$

where

$$\begin{aligned} \Xi^{(q)} &= [\mathbf{H}_{L-1}^{(q)} \ \mathbf{H}_{L-2}^{(q)} \ \dots \ \mathbf{H}_{0}^{(q)}] \\ &\times \begin{pmatrix} \mathbf{x}^{(q)}(nP) & \dots & \mathbf{x}^{(q)}((n-K+1)P+P-L) \\ \vdots & \ddots & \vdots \\ \mathbf{x}^{(q)}(nP+L-1) & \dots & \mathbf{x}^{(q)}((n-K+1)P+P-1) \end{pmatrix} \end{aligned} \tag{3.51}$$

$$\begin{aligned} \Rightarrow \ \Xi^{(q)} &= [\mathbf{R}_{r,L-1}^{1/2}\mathbf{H}_{w,L-1}^{(q)} \ \mathbf{R}_{r,L-2}^{1/2}\mathbf{H}_{w,L-2}^{(q)} \ \dots \ \mathbf{R}_{r,0}^{1/2}\mathbf{H}_{w,0}^{(q)}] \\ &\times \begin{pmatrix} \mathbf{R}_{t,L-1}^{1/2\,(q)} & \dots & \mathbf{0} \\ \vdots & \ddots & \vdots \\ \mathbf{0} & \dots & \mathbf{R}_{t,0}^{1/2\,(q)} \end{pmatrix} \\ &\times \begin{pmatrix} \mathbf{x}^{(q)}(nP) & \dots & \mathbf{x}^{(q)}((n-K+1)P+P-L) \\ \vdots & \ddots & \vdots \\ \mathbf{x}^{(q)}(nP+L-1) & \dots & \mathbf{x}^{(q)}((n-K+1)P+P-1) \end{pmatrix} \end{aligned} \tag{3.52}$$

We note that in eq.s (3.51) and (3.52), even though the block channel matrix between the qth interferer and the desired user is of order, say L_q, the interference is observed only over L lags of the intended channel. Also, the receive correlation matrices are still, $\mathbf{R}_{r,l}^{1/2}$.

$$\begin{aligned} \Rightarrow \ \Xi^{(q)} &= [\mathbf{R}_{r,L-1}^{1/2} \ \mathbf{R}_{r,L-2}^{1/2} \ \dots \ \mathbf{R}_{r,0}^{1/2}] \times \begin{pmatrix} \mathbf{H}_{w,L-1}^{(q)} & \dots & \mathbf{0} \\ \vdots & \ddots & \vdots \\ \mathbf{0} & \dots & \mathbf{H}_{w,0}^{(q)} \end{pmatrix} \\ &\times \begin{pmatrix} \hat{\mathbf{x}}^{(q)}(nP) & \dots & \hat{\mathbf{x}}^{(q)}((n-K+1)P+P-L) \\ \vdots & \ddots & \vdots \\ \hat{\mathbf{x}}^{(q)}(nP+L-1) & \dots & \hat{\mathbf{x}}^{(q)}((n-K+1)P+P-1) \end{pmatrix} \end{aligned} \tag{3.53}$$

where,

$$\hat{\mathbf{x}}^{(q)}((n-k)P+p-l) = \mathbf{R}_{t,l}^{1/2\,(q)}\mathbf{x}^{(q)}((n-k)P+p-l) \tag{3.54}$$

$$\begin{aligned}\Rightarrow \quad \Xi^{(q)} &= \underbrace{[\mathbf{R}_{r,L-1}^{1/2} \;\; \mathbf{R}_{r,L-2}^{1/2} \;\; ... \;\; \mathbf{R}_{r,0}^{1/2}]}_{\triangleq \mathbf{R}_r^{1/2}} \\ \times \quad &\underbrace{\begin{pmatrix} \mathbf{H}_{w,L-1}^{(q)}\hat{\mathbf{x}}^{(q)}(nP) & \dots & \mathbf{H}_{w,L-1}^{(q)}\hat{\mathbf{x}}^{(q)}((n-K+1)P+P-L) \\ \vdots & \ddots & \vdots \\ \mathbf{H}_{w,0}^{(q)}\hat{\mathbf{x}}^{(q)}(nP+L-1) & \dots & \mathbf{H}_{w,0}^{(q)}\hat{\mathbf{x}}^{(q)}((n-K+1)P+P-1) \end{pmatrix}}_{\triangleq \mathcal{H}(\hat{\mathbf{y}}^{(q)})}\end{aligned} \tag{3.55}$$

By applying again, the vectorization equality, (𝕀1), we have,

$$\boldsymbol{\Xi}^{(q)} = vec\,(\Xi^{(q)}) = (\,\mathrm{I}_{(KP-L)\times(KP-L)} \otimes \mathbf{R}_r^{1/2}\,)\,\underbrace{vec\,(\mathcal{H}(\hat{\mathbf{y}}^{(q)}))}_{\triangleq\, \hat{\mathbf{y}}^{(q)}} \tag{3.56}$$

The covariance matrix of $\boldsymbol{\Xi}^{(q)}$ is now given as,

$$\begin{aligned}\mathbf{R}_{\boldsymbol{\Xi}}^{(q)} &= \mathrm{E}\{\,(\,\mathrm{I}_{(KP-L)\times(KP-L)} \otimes \mathbf{R}_r^{1/2}\,)\hat{\mathbf{y}}^{(q)} \\ &\times \quad (\hat{\mathbf{y}}^{(q)})^{\mathrm{H}}(\,\mathrm{I}_{(KP-L)\times(KP-L)} \otimes \mathbf{R}_r^{1/2}\,)^{\mathrm{H}}\,\} \qquad (3.57) \\ &= (\,\mathrm{I}_{(KP-L)\times(KP-L)} \otimes \mathbf{R}_r^{1/2}\,)\,\mathrm{E}\{\,\hat{\mathbf{y}}^{(q)}(\hat{\mathbf{y}}^{(q)})^{\mathrm{H}}\} \\ &\quad (\,\mathrm{I}_{(KP-L)\times(KP-L)} \otimes (\mathbf{R}_r^{1/2})^{\mathrm{H}}\,) \qquad (3.58)\end{aligned}$$

where,

$$\begin{aligned}&\mathrm{E} \;\; \{\,\hat{\mathbf{y}}^{(q)}(\hat{\mathbf{y}}^{(q)})^{\mathrm{H}}\} = \\ &\begin{pmatrix} \sum_{j=1}^{N_t} R_{j,j}^{(q),n}(0)\mathbf{I}_{LN_r} & \dots & \sum_{j=1}^{N_t} R_{j,j}^{(q),n-K+1}(P-L)\mathbf{I}_{LN_r} \\ \vdots & \ddots & \vdots \\ \sum_{j=1}^{N_t} R_{j,j}^{(q),n}(L-1)\mathbf{I}_{LN_r} & \dots & \sum_{j=1}^{N_t} R_{j,j}^{(q),n-K+1}(P-1)\mathbf{I}_{LN_r} \end{pmatrix} \qquad (3.59) \\ &\Rightarrow \mathrm{E}\{\,\hat{\mathbf{y}}^{(q)}(\hat{\mathbf{y}}^{(q)})^{\mathrm{H}}\} = \mathbf{R}_{\hat{\mathbf{y}}}^{(q)} \otimes \mathbf{I}_{LN_r} \qquad (3.60)\end{aligned}$$

Therefore,

$$\begin{aligned}\mathbf{R}_{\boldsymbol{\Xi}}^{(q)} &= (\,\mathrm{I}_{(KP-L)\times(KP-L)} \otimes \mathbf{R}_r^{1/2}\,)\,(\mathbf{R}_{\hat{\mathbf{y}}}^{(q)} \otimes \mathbf{I}_{LN_r}) \\ &\quad (\,\mathrm{I}_{(KP-L)\times(KP-L)} \otimes (\mathbf{R}_r^{1/2})^{\mathrm{H}}\,) \qquad (3.61) \\ \Rightarrow \mathbf{R}_{\boldsymbol{\Xi}}^{(q)} &= \mathbf{R}_{\hat{\mathbf{y}}}^{(q)} \otimes \mathbf{R}_r \qquad (3.62)\end{aligned}$$

which is obtained by applying the vectorization equality, (𝕀2). Finally,

$$\mathbf{R}_{\boldsymbol{\Xi}} = \sum_{q=1}^{Q} \mathbf{R}_{\boldsymbol{\Xi}}^{(q)} = \sum_{q=1}^{Q} \mathbf{R}_{\hat{\mathbf{y}}}^{(q)} \otimes \mathbf{R}_r = \mathbf{R}_{\hat{\mathbf{y}}}^{(Q)} \otimes \mathbf{R}_r \tag{3.63}$$

with the last equality obtained due to (𝕀3). □

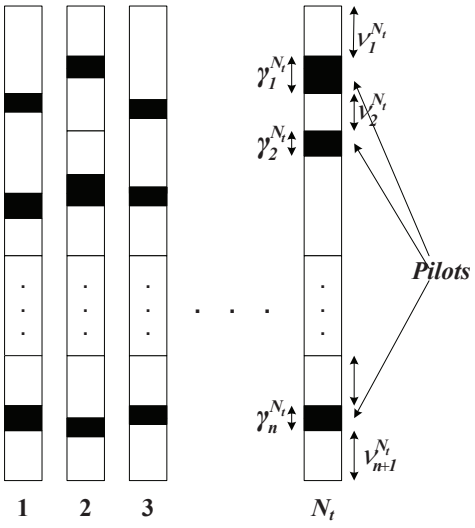

Figure 3.2: Data packets across J transmit antennas each with multiple pilot clusters

3.5.2 Optimal Training Design

Based on the FIM derived in the above sections both for the deterministic and random unknown parameter cases, our aim is to optimally design the training symbol matrix. Our goal will also involve their optimal placement which will be known to the transmitter as well as the receiver. An illustration of the optimal training symbol matrix as shown in Figure 3.2.

Chapter 4

BLISS-enabled Hardware Prototype

4.1 Introduction: Antenna Subset Selector Board

The Antenna Subset Selection (AntSS) system consists of a series of AntSS boards that provides 2^M-to-2^N downselection from an array of receive antennas to a set of BLISS receiver inputs. Each individual AntSS board provides 4-to-2 antenna downselection via a set of RF switches. A basic block diagram of an individual AntSS board is given in Figure 4.1. Each AntSS board has four receive paths. Each path consists of a bandpass filter and low-noise amplifier. The output of each receive path is connected to a switch matrix composed of a series of Single-Pole-Double-Throw (SPDT) RF Switches. The switch matrix is configured so that all possible permutations of the 4-to-2 downselection are possible. The switch matrix is controlled by software running on a simple PIC processor. The PIC interfaces with the BLISS hardware platform via an RS-232 link that is connected from the BLISS receiver to all AntSS boards.

4.2 Operation of a Single AntSS Board

Each AntSS board has a unique identifier (described below) that will allow it to communication with the BLISS control PC. Upon power-up, each board will broadcast its unique 9-bit Board ID (BID) on the Common Control/Data Bus (CCDB). The BLISS Control Software (BCS) will log the ID and send an acknowledge signal back to the originating AntSS Board. If the AntSS board does not receive a positive acknowledgement, after a random timeout, it will rebroadcast its ID, and continue to do so until it receives an acknowledge from the BCS. After receiving the acknowledge signal, the AntSS board will configure itself into a default state, with Antenna "A" connected to "Path 1" and Antenna "B" connected to "Path 2". Additionally, each board will then enter an "Address Detection Mode" where they ignore all communication that is not 9-bits long (potentially allowing the BCS to utilize the CCDB for communication to other, non-AntSS devices). Communication with an individual AntSS board involves the following steps:

1. The BCS sends out a 9-bit BID on the CCDB which is the address of the AntSS board it desires to communicate with.

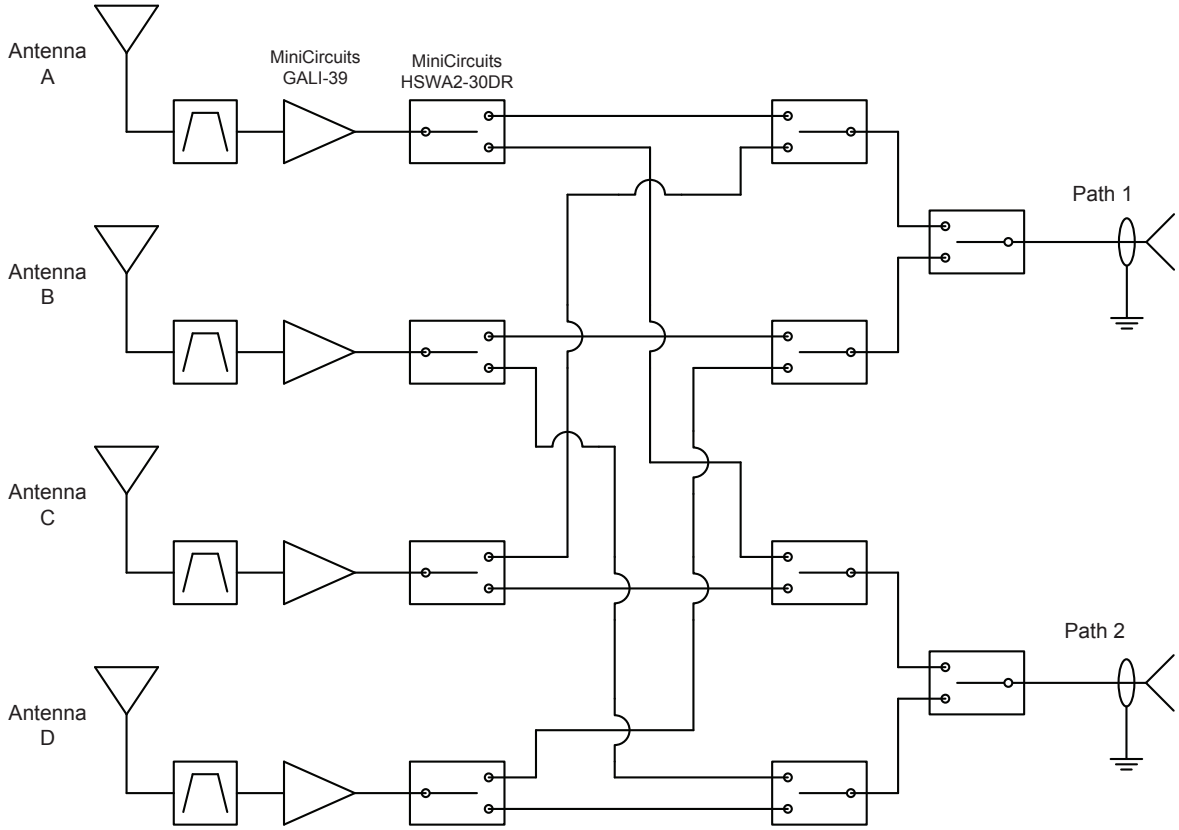

Figure 4.1: AntSS Board Block Diagram

2. All AntSS boards connected to the CCDB decode the BID, and the AntSS board with the matching BID drops out of "Address Detection Mode" and enters "Command and Control Mode".

3. The BCS then sends one of the valid commands described below. All AntSS boards except the one in "Command and Control Mode" ignore the communication.

4. To indicate the end of a command, the BCS sends a double-stop (Carriage Return/Line Feed), which indicates that communication is finished. The AntSS board then processes the command, re-enters "Address Detection Mode", and sends a positive acknowledge to the BCS.

In addition to the commands described below, the all-ones BID is reserved to initiate a Board ID Scan. When receiving this BID, the AntSS board will re-report its BID to the BCS using the start-up procedure described above. This command differs from the power-on startup in that it does not change the configuration of the Antenna Switch Matrix.

Commands and data on the CCDB are formatted as ASCII text characters for ease of debugging and understanding. At the current time, valid commands consist of:

- SRB: Soft Reboot. Puts each board back into the initial power-up state, and will cause the boards to revert back to the default antenna configuration.

- SSM WXYZ: Set Switch Matrix. Configures the switch matrix to downselct a desired set of antennas. The characters "W" and "Y" determine which of the four input antennas will be selected, and the characters "X" and "Z" determine which of the output paths the antennas will be mapped to. For example, "A1C2" tells the AntSS board to map Antenna A to Path 1 and Antenna C to Path 2.

- RSM WXYZ: Read Switch Matrix. Reports the current state of the switch matrix. The AntSS board reports back the "WXYZ" code described above that contains the current status of the Switch Matrix.

4.3 AntSS Board Hierarchy

To achieve greater diversity in antenna selection, individual AntSS boards may be connected together in a Tree hierarchy, as shown below in Figure 4.2. The primary limitation is the complexity of the interconnection on the hierarchy, as it grows exponentially with the number of levels. To identify a particular board in the hierarchy, each board is assigned a specific two-digit BID, as illustrated in Figure 4.2. The first digit represents the Level in the hierarchy, and the second represents the block of antennas the board is physically connected to. To avoid confusion, input antennas for a given board are also referred to by an alphanumeric identifier consisting of a number followed by a group of letters. The number represents the level of the hierarchy, and the alpha code represents the antennas position in the heierarcy. To illustrate, BID 0-0 is the AntSS board at the very first level in the hierarchy, and is connected to just four input antennas: 0A, 0B, 0C, and 0D. AntSS Board 3-1 is at the fourth level in the hierarchy and is connected to input antennas 3A, 3B, 3C, and 3D; Board 3-7 is also at the fourth level of the hierarchy and is connected to input antennas 3AC, 3AD, 3AE, and 3AF. As mentioned above, each board has a unique 9-bit BID, the contents of which are illustrated in Figure 4.3 and described below.

The current addressing scheme supports up to 256-to-2 Antenna Subset selection. For 256 input antennas, the hierarchy requires six (6) levels, thus bits B_8-B_6 in the BID determine which level the AntSS board is located in. At level 6, 64 boards are required to handle the 256 input antennas. Thus, bits B_5-B_0 determine which group of input antennas each board is physically connected to. For Example, BID "000000000" would be assigned to the board at Level 0, and input antennas 0A-0D. BID "110000000" is the board at Level 6, antennas 6A-6D; BID "110111111" is at Level 6, antennas 256-253 (whatever alpha code that works out to be).

The first bit in the identifier is the hierarchy number. Currently, the addressing scheme supports two different hierarchies, each of which can have up to 256-to-2 antenna subset selection. Thus, Bit 8 in the addressing scheme represents the hierarchy number. To achieve 512-to-2 downselection requires 8 levels, thus, bits B7-B5 determine which level in the hierarchy the board is located at.

Table 4.1: AntSS Selection Matrix

Antenna	BER	SINR	γ	α
N_1				
A_1				
$\vdots$				
N_N				
A_N				

4.4 BLISS AntSS Operation

The BLISS AntSS Algorithm operates off of training data that is broadcast during data communications. The training data serves a dual purpose: estimate Channel State Information for the BLISS blind source separation, and estimate (using the metrics described below) which antennas provide the highest quality communication link. When called, the AntSS algorithm initiates a scan of the entire antenna hierarchy. For each of the K antennas in the hierarchy, the AntSS algorithm calculates the following metrics:

- Normalized Bit Error Rate: $BER_i = min(BER)/BER_i$
  where BER_i is the calculated BER for the ith antenna, $min(BER)$ is the minimum BER across all antennas, and BER_i is the BER metric, and varies from 01. A 0 represents the worst-possible BER, and 1 represents the best possible BER.

- Normalized SINR: $SINR_i = SINR_i/max(SINR)$
  where $SINR_i$ is the calculated SINR for the ith antenna, $max(SINR)$ is the maximum SINR as measured across all antennas, and $SINR_i$ is the SINR metric, and varies from 01. A 0 represents the worst possible SINR, a 1 represents the best possible SINR.

- Normalized Fading Metric: $\gamma_i = \gamma_i/min(\gamma)$
  where γ_i is the calculated Fading Metric for the ith antenna. At the current time, the exact determination of the Fading Metric is unknown, but two possibilities exist. The first is to use the Mean Square Error between the blindly estimated channel state information and the true channel state information (assuming it is available). The second is to evaluate the number of burst errors and/or drops in Received Signal Strength, to determine how rapidly the received signal fluctuates. min is the worst-possible fading metric across all antennas, and γ_i is the Fading metric, and varies from 01. A 0 represents the maximum possible level of fading, and a 1 represents the minimum possible level of fading.

- Weighted Sum of Metrics: $\alpha_i = w_1 \times BER_i + w_2 \times SINR_i + w_3 \times \gamma_i$
  The AntSS algorithm then constructs a Selection Matrix of the metrics, as illustrated below: Based on this Selection Matrix, the end user can determine how they want the AntSS algorithm to optimize the antenna selection. For example, the user could choose to optimize based on BER, in which case, the AntSS algorithm would simply select the two antennas that have the best BER. Or, the end user could choose to optimize BER subject to a SINR that is greater than a threshold, and/or subject to fading

less than a threshold. The user could also choose to optimize based on the weighted summationthis technique would be advantageous in a highly dynamic environment where channel parameters are rapidly varying.

4.5 Antenna Subset Selector Board : Implementation

Figures 4.4, 4.5, and 4.6 provide the schematics for the AntSS board as implemented by the US Naval Academys Wireless Measurements Group. Figure 4.7 is an image of a fully constructed AntSS board. In order to validate the performance of the AntSS board, each of the individual RF paths were characterized using the Wireless Measurements Group Agilent E8XXXXX Vector Network Analyzer. Figures 4.8, 4.9, 4.10, 4.11, 4.12, 4.13, 4.14, and 4.15 show the measured S21 performance for each Path. Figure 4.16 shows a comparison of the S21 performance among all paths. From the figures, we observe that the 3dB bandwidth of the AntSS board is approximately 1.8 GHz, which is slightly less than the designed value of 2.2 GHz that would match the tuning range of the Ettus Research WBX board. We also observe that the gain is relatively flat over the 3 dB bandwidth, varying by less than 0.25 dB. Looking at the comparison figure (Figure 4.16), we observe that, over the 3 dB bandwidth, the gains among the various RF paths vary by less than 1 dB, meaning that the paths have an excellent degree of gain matching. Beyond the 3 dB bandwidth, the AntSS board still proves some gain, up to a maximum frequency of 3.0 GHz. However, when operating between 1.8 and 3.2 GHz, the performance of the RF paths varies considerably, and care must be taken to account for the variable gains in the Selection Matrix.

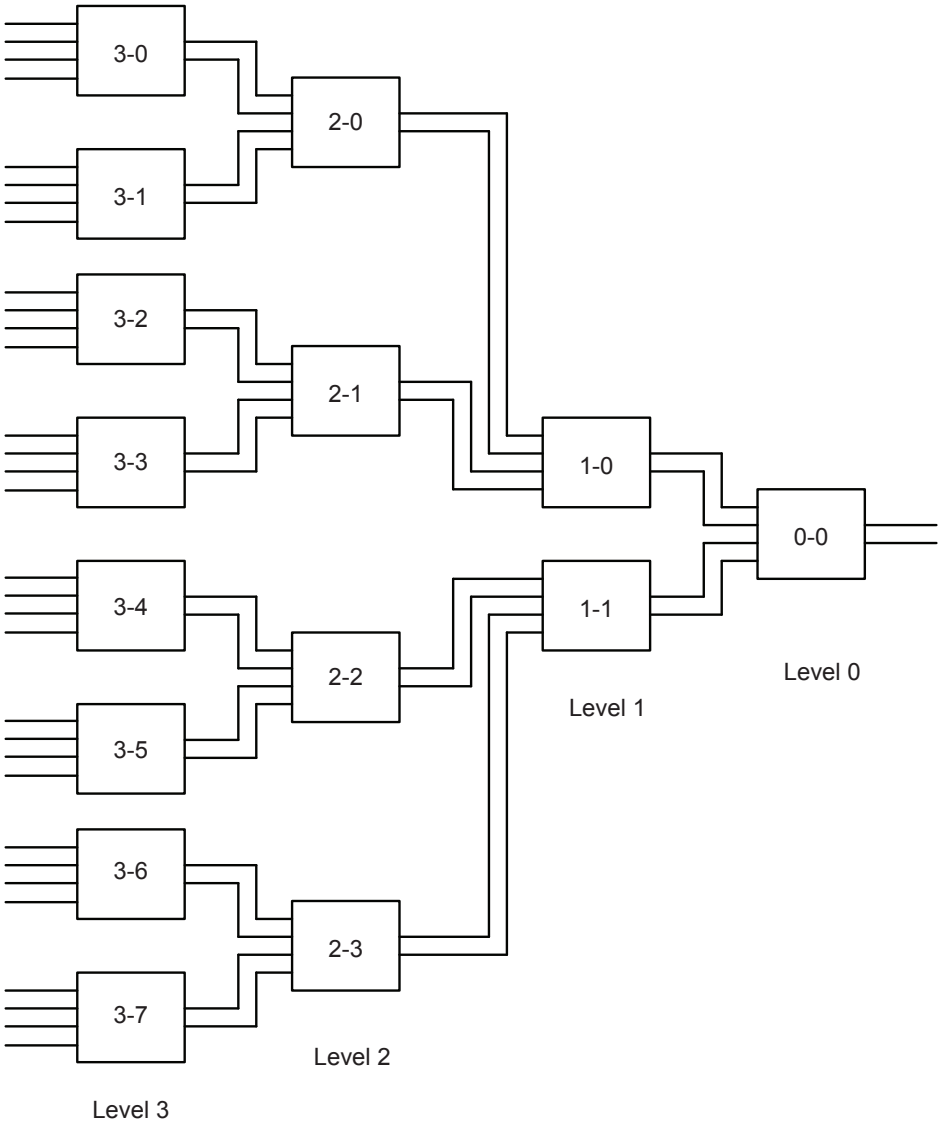

Figure 4.2: AntSS Hierarchy for 2^N-to-2 Antenna Downselection. Illustrated is a 32-to-2 downselection

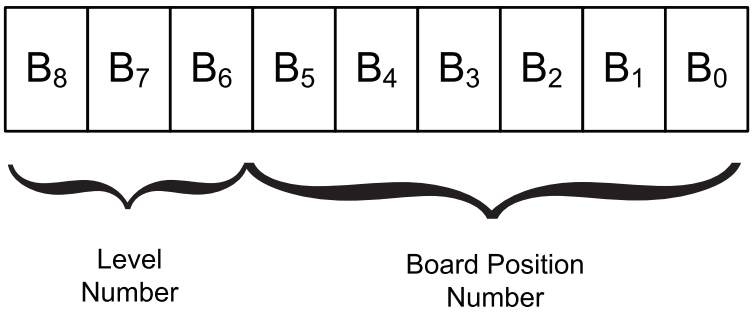

Figure 4.3: The 9-bit Board Identifier (BID) Illustrated

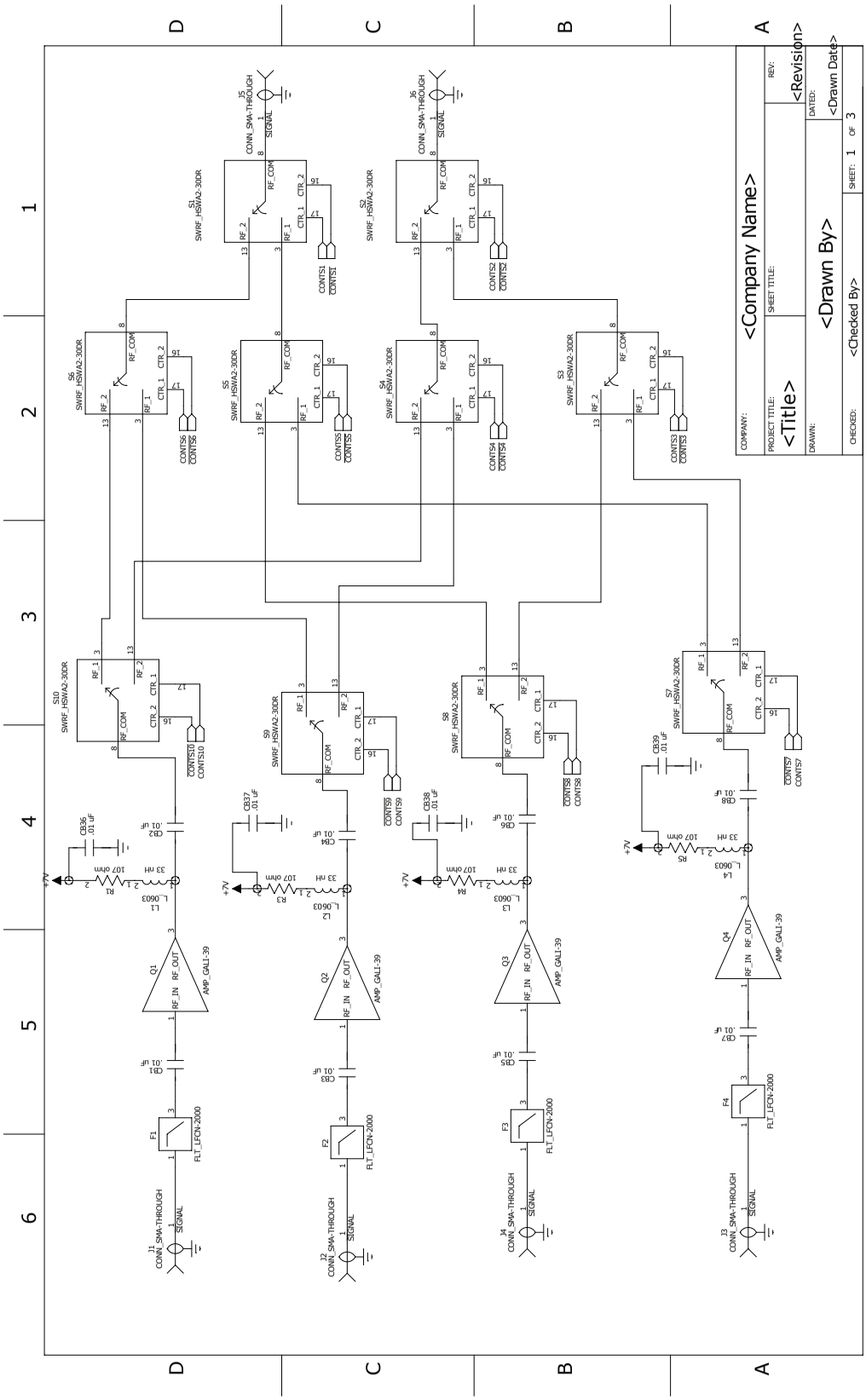

Figure 4.4: Schematic for the AntSS Board

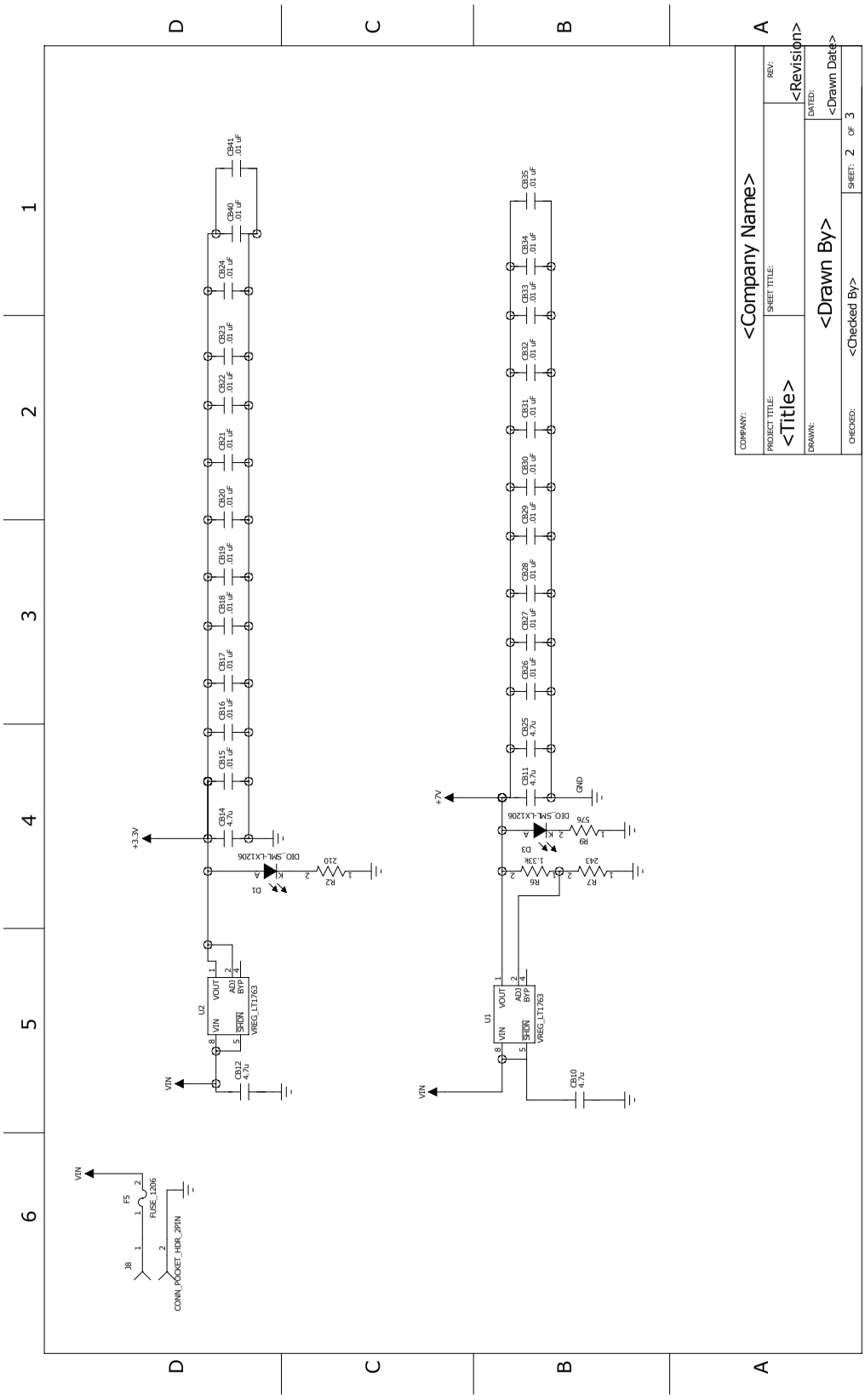

Figure 4.5: Schematic for the AntSS Board

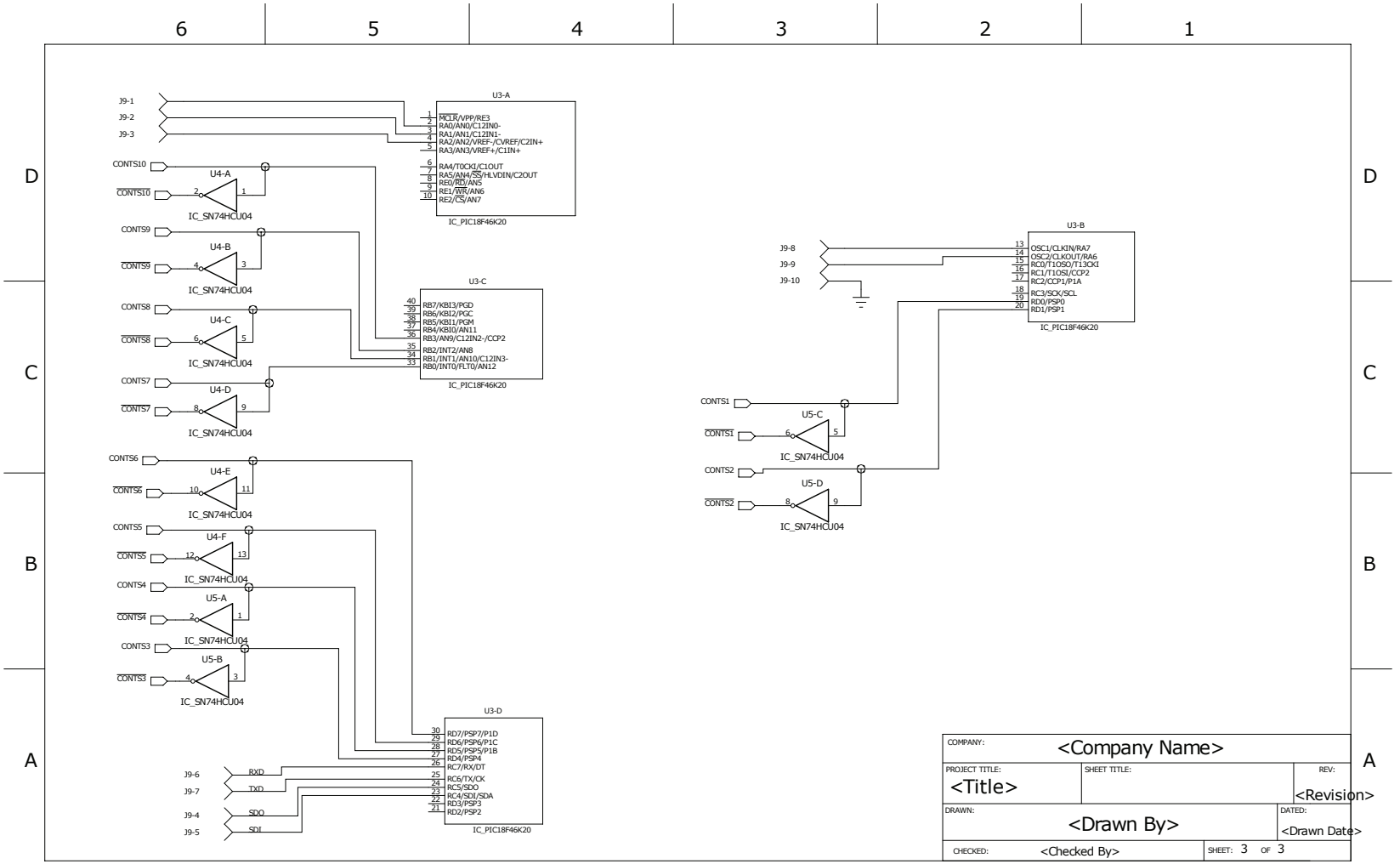

Figure 4.6: Schematic for the AntSS Board

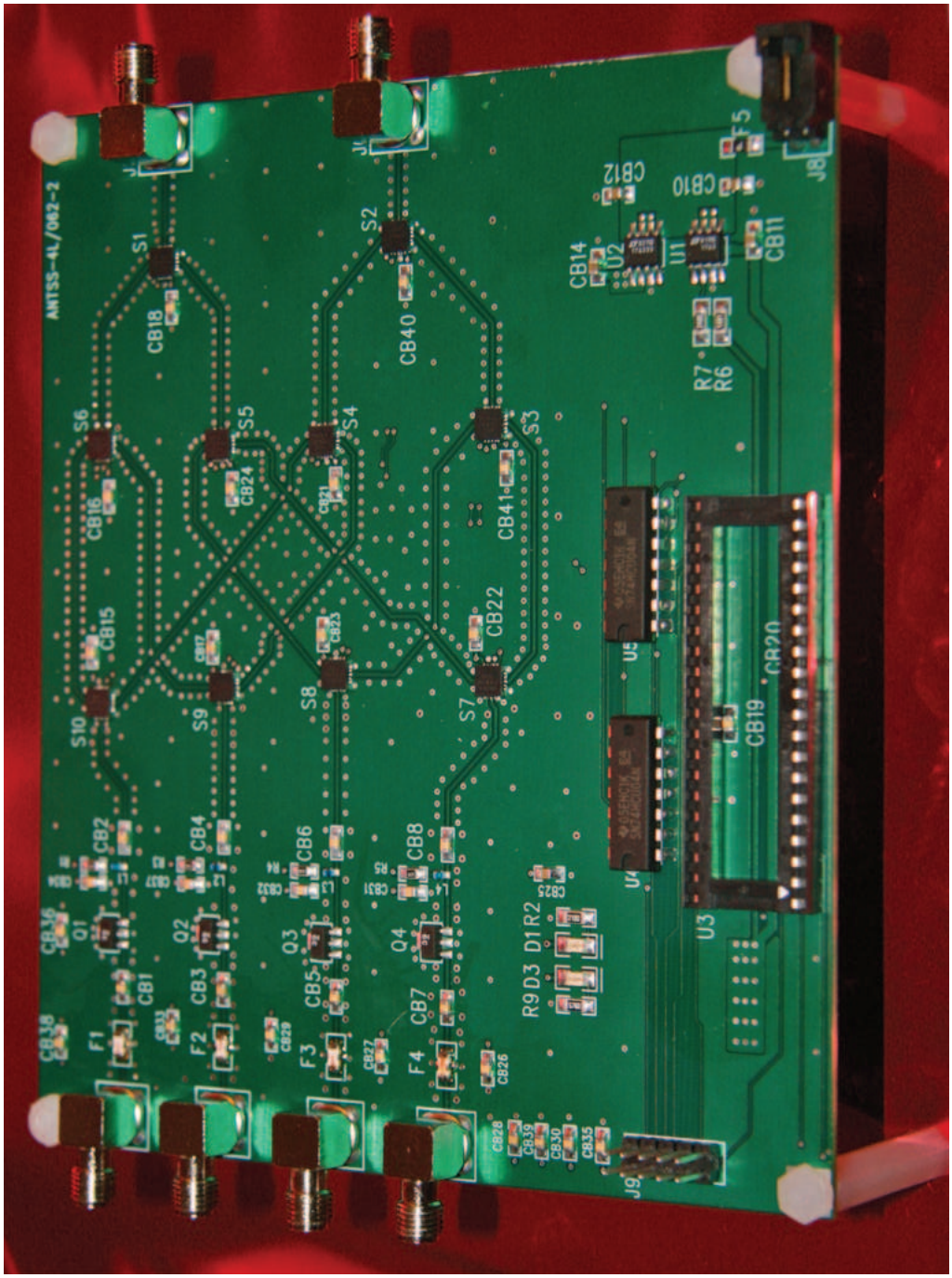

Figure 4.7: An image of the constructed AntSS Board

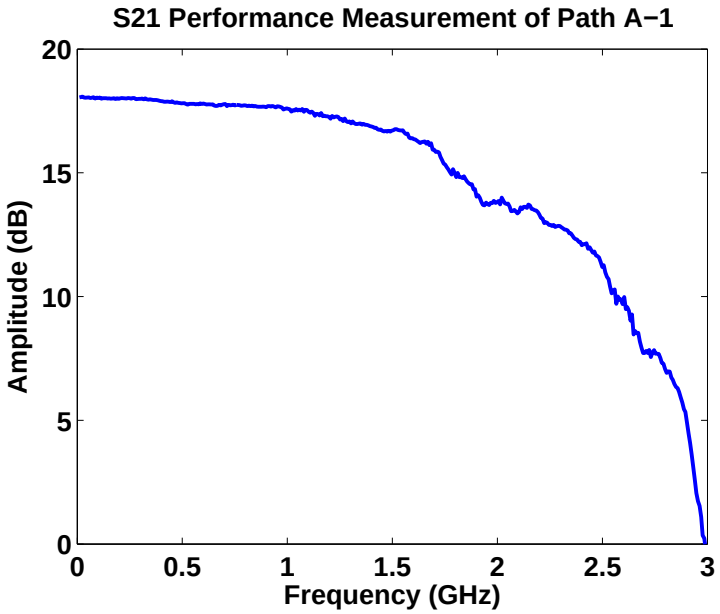

Figure 4.8: The measured S21 performance for Path $A-1$

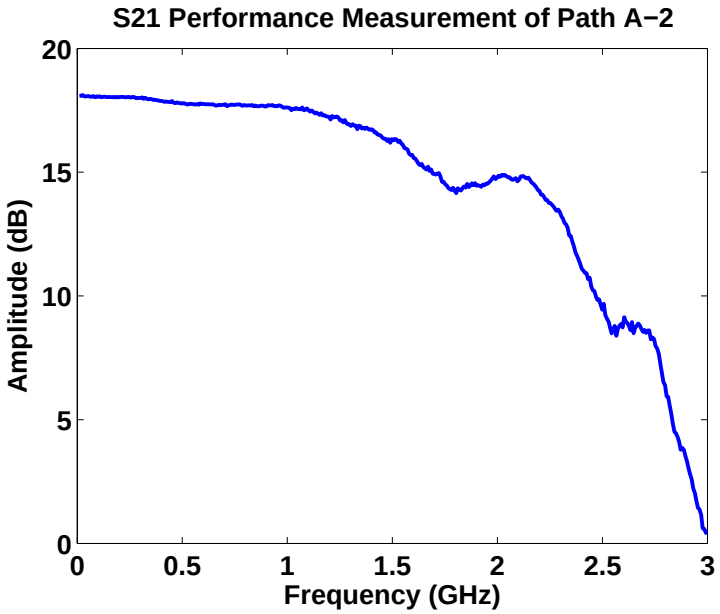

Figure 4.9: The measured S21 performance for Path $A-2$

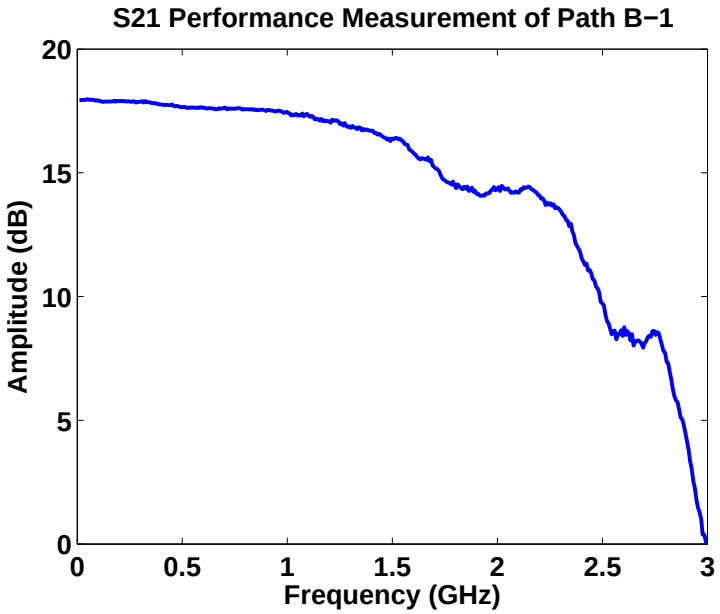

Figure 4.10: The measured S21 performance for Path $B-1$

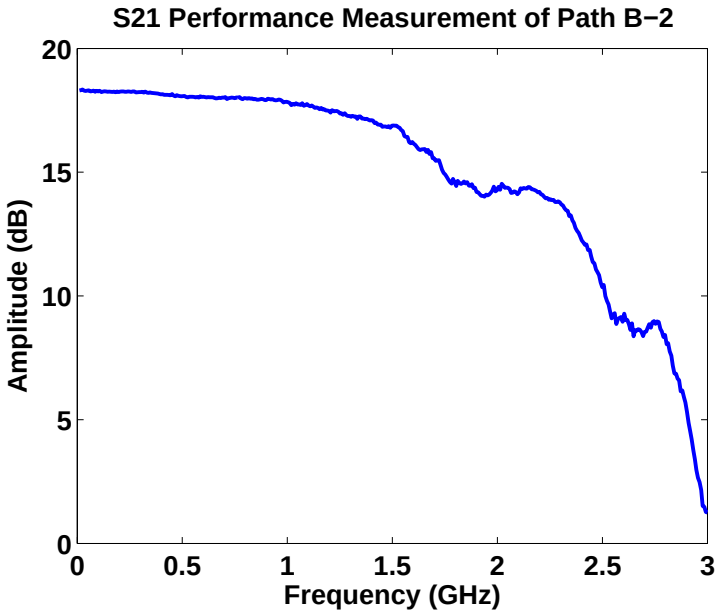

Figure 4.11: The measured S21 performance for Path $B-2$

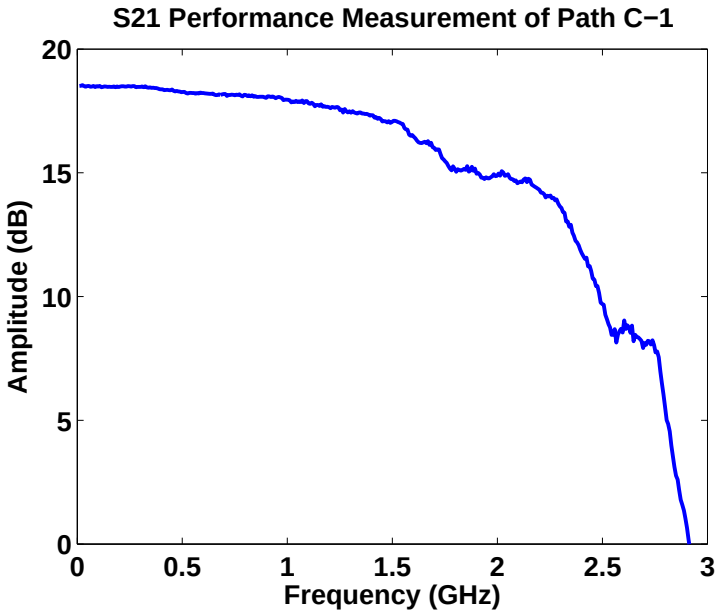

Figure 4.12: The measured S21 performance for Path $C-1$

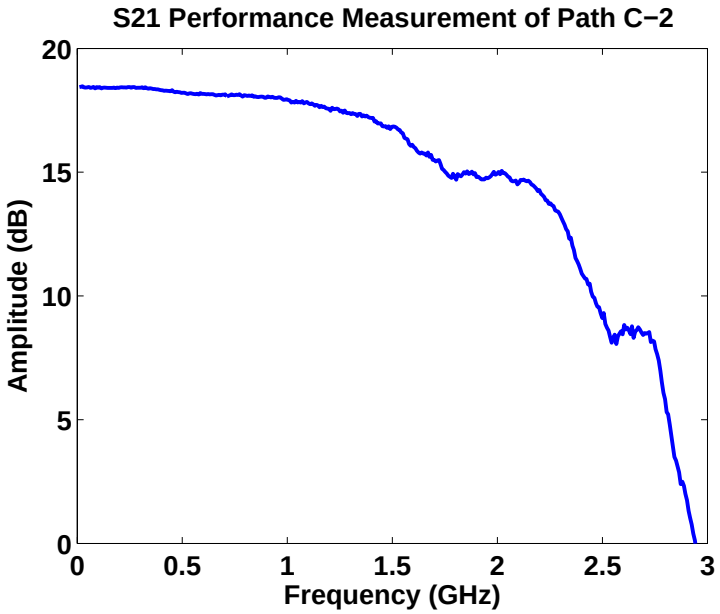

Figure 4.13: The measured S21 performance for Path $C-2$

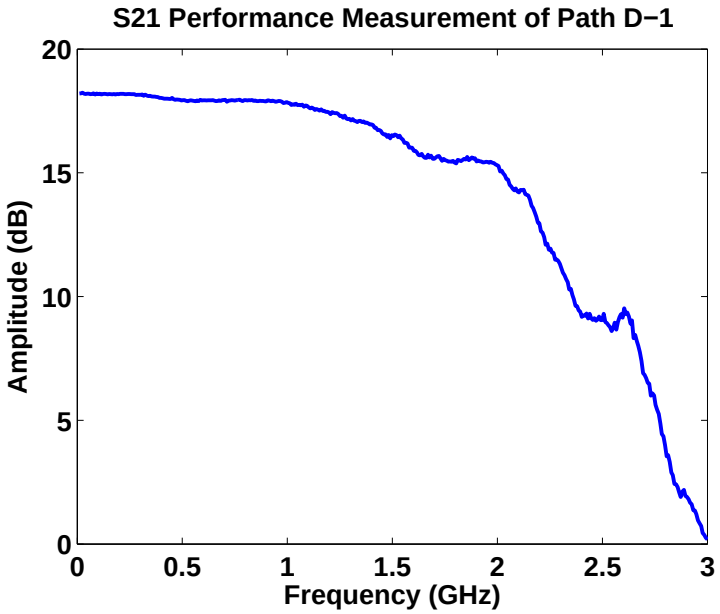

Figure 4.14: The measured S21 performance for Path $D-1$

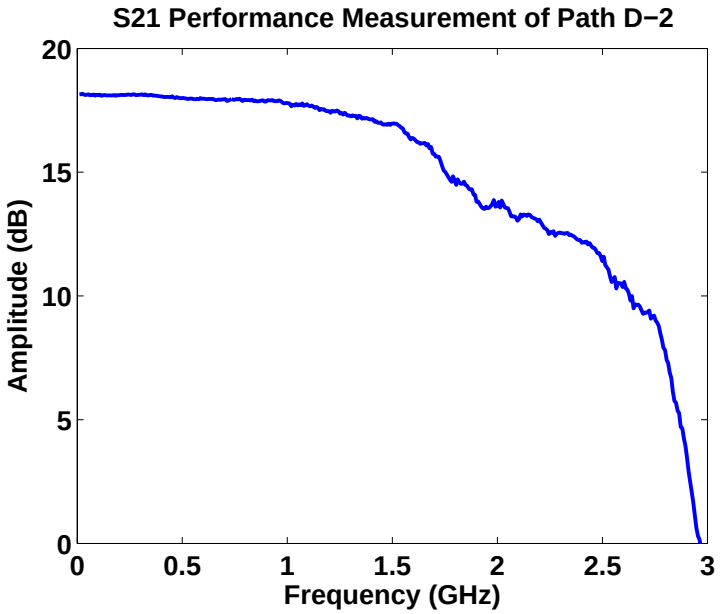

Figure 4.15: The measured S21 performance for Path $D-2$

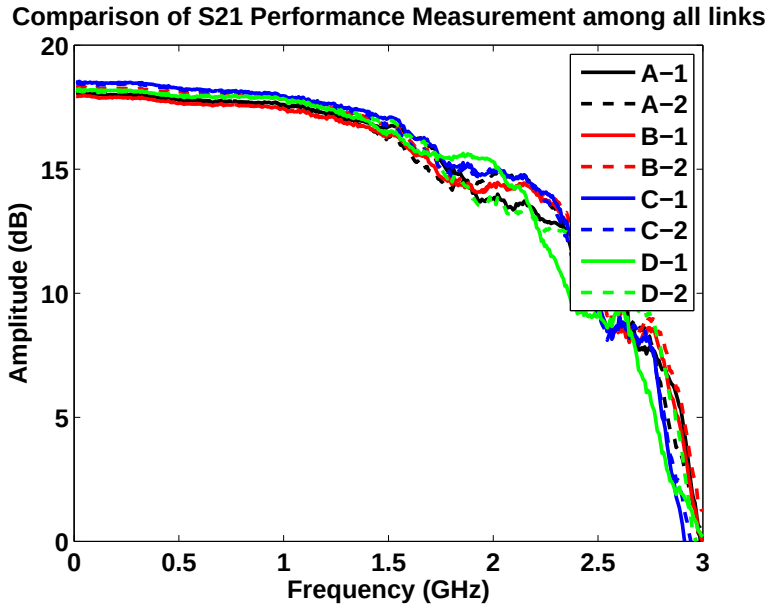

Figure 4.16: A comparison of the S21 performance among all paths

Appendix A

2011 IEEE ICASSP Conference Paper Submission – Reviewer Feedback

The following email is a collection of the anonymous reviewer feedback regarding our conference paper submission to the 2011 IEEE International Conference on Acoustics, Speech, and Signal Processing (2011 IEEE ICASSP) received on 17 January 2011 [1]. Although the paper was declined for presentation at this conference (acceptance rate = 50%), much of the reviewer feedback was positive in terms of the timeliness and importance of this research that is being pursued through this project.

Some of the factors that affected the acceptance of this paper included the lack of details due to space constraints, the lack of experimental results (note that the blind source separation component of this work is primarily theoretical), and several formatting/consistency issues. Nevertheless, the reviewers felt that this work was interesting and much of their feedback focused on how to further enhance the presentation of this paper for resubmission to another peer-reviewed conference venue.

```
-----Original Message-----
From: ICASSP 2011 Notifications [mailto:papers@icassp2011.com] Sent:
Monday, January 17, 2011 3:59 PM To: srikanthp@WPI.EDU;
alexw@WPI.EDU; canderso@usna.edu Subject: ICASSP 2011 Review Results
for paper #3853 Importance: High

Dear Srikanth Pagadarai, Alexander Wyglinski, Christopher Anderson

Paper ID: 3853 Title: 'REGULARITY IN INTERFERENCE-LIMITED MIMO
COMMUNICATIONS UNDER BASIS FUNCTION CONSTRAINTS'

Thank you for submitting the above listed manuscript for
consideration for inclusion in the ICASSP 2011 program.  We regret
to inform you that your paper has not been accepted for presentation
at the conference.  The reviewers' comments on your paper are
attached at the end of this email.  These comments served as part of
the basis for the Technical Committee's decision and may offer
```

useful feedback that can be used to strengthen your future publication submissions.

The Technical Program Committee carefully selected reviewers for ICASSP 2011 and assigned reviewers papers in their areas of expertise. Every paper received at least two reviews. This year we received a record number of 3018 papers and were only able to accept 1500. The Technical Program Committee worked very hard to place as many excellent papers into the program as possible, but the competition was severe and some very good papers were rejected.

While we recognize that this information is disappointing to you, we would encourage you to attend the conference and to enter into discussion with authors whose papers are in your field of interest. Information on many aspects of ICASSP 2011, including the venue, accomodation, tourism, and visa requirements, are available on the conference web site http://www.icassp2011.com, and more will be available soon. The complete technical program will be listed shortly.

In about two weeks, you will receive an e-mail announcing the opening of the registration website. For those who will need a visa, please note that the IEEE has strict guidelines that invitation letters for visa purposes can only be sent to people who have completed the registration process. Further information regarding invitation letters is posted on the website, see http://www.icassp2011.com/en/general-info/good-to-know/passport-and-visa-requirements Please note that the visa application procedure can take up to two months.

We look forward to welcoming you in Prague, Czech Republic, in May.

Sincerely,

Alle-Jan van der Veen and Jonathon Chambers ICASSP 2011 Technical Program Co-Chairs

---- Comments from the Reviewers: ----
Importance/Relevance: Of sufficient interest Comment on Importance/Relevance: The basic work in this paper is the derivation of the Fisher information matrix and ways of making it invertible. This is too special a topic to be "of broad interest", but maybe some readers will be interested. Also, most of the presentation is consumed by introducing the model and doing some tedious

calculations with it. There are no new techniques or surprising results.

Novelty/Originality: Minor originality Comment on Novelty/Originality: Most of the presentation is consumed by introducing the model and doing some tedious calculations with it. There are no new techniques or surprising results. Many key steps have been derived in previouas papers by different authors.

Technical Correctness: Probably correct Comment on Technical Correctness: The space is too resticted to perform all the necessary calculations. Many of the steps that have been left out should be obvious to experts.

Experimental Validation: Sufficient validation/theoretical paper Comment on Experimental Validation: There is no need for experimental validation in this paper.

Clarity of Presentation: Difficult to read Comment on Clarity of Presentation: Much of the notation is not introduced properly. This also implies in some cases that a concept is not understood until later in the paper, where the meaning of a symbol can be inferred from the context. Here comes a list: - lower case boldface letters mean the vectorized form of the corresponding upper case matrix objects, - W_n is not introduced in (4), but only later, - you explain what boldface \bar H_l means even though it is not introduced in (5), but only later, - mention that K\leq L, - the fact that boldface \ddot Y_n=boldface \dot Y_n may lead to misunderstandings; why not call it \hat Y_n and the two different versions y_n(1)} and y_n(2)}, respectively? - mention that L_q\leq P, as far as I understand, eq.s (14a) and (14b) imply that H is assumed to be Gaussian. which has not been mentioned before in the paper, - the notation of the vector [x^T -h^T 0^t] is very misleading, maybe you should at least write (-h^T), - as far as I understand the proof of Theorem 1, the second papragraph deals with the case N_t\geq 2, but this is not mentioned anywhere, - in (17), the first = should not be there, that's it.

Reference to Prior Work: References adequate

Importance/Relevance: Of limited interest Comment on Importance/Relevance: see below

Novelty/Originality: Moderately original

Technical Correctness: Probably correct

Experimental Validation: Insufficient validation Comment on Experimental Validation: there are no numerical results

Clarity of Presentation: Difficult to read Comment on Clarity of Presentation: see below

Reference to Prior Work: References missing Comment on Reference to Prior Work: see below

General Comments to Authors: The paper analysis semi-blind channel estimation in MIMO interference-limited systems based on the assumption of a single known precoder for all the transmitting nodes in the network. The authors first highlight the importance of (semi-)blind channel estimation and then show that under certain conditions semi-blind channel estimation is theoretically possible by only knowing the precoder of the multiple-antenna equipped nodes in the network.

The system model, however, is not well defined, the introduction is not fully relevant to the problem the paper is addressing, the references are out-dated and there are no numerical analysis validating the analysis of the paper. Moreover, some of the main assumption of the paper are not well justified, for example, the authors assume all the transmitting nodes are using the same precoder, which is hardly the case in current and future heterogeneous interference-limited MIMO networks. The authors could use the extra space to elaborate on the problem they are solving or present numerical analysis.

Importance/Relevance: Of sufficient interest

Novelty/Originality: Moderately original

Technical Correctness: Probably correct

Experimental Validation: Limited but convincing

Clarity of Presentation: Difficult to read Comment on Clarity of Presentation: See below.

Reference to Prior Work: References adequate

General Comments to Authors: This paper considers a Multi user MIMO setup operating over frequency selective block fading channels, where a MIMO link of interest is corrupted by MIMO interferers. Blind system identification is investigated, and more exactly the issue is the Fisher Information Matrix (FIM) of the data, channel and interference which is rank deficient. Data precoding is assumed, with the same precoder for all links. The analysis conducted is to investigate how the use of the basis functions or precoder constraints can be used to restore the rank of the FIM.

The topic is very interesting. The paper however is a bit disappointing in several aspects. - It seems to have been written in a hurry and lacks a discussion at the end or strong conclusions. - Reading the last sentence (containing equation 23) one expects something after, but the paper stops ! - A number of assumptions should have been discussed, like for instance is it reasonable to assume that all users will use the same precoding matrix.

Bibliography

[1] S. Pagadarai, A. M. Wyglinski, and C. R. Anderson, "Regularity in interference-limited MIMO communications under basis function constraints," in *IEEE International Conference on Acoustics, Speech, and Signal Processing*, 2011. Submitted.

[2] G. J. Foschini and M. J. Gans, "On Limits of Wireless Communications in a Fading Environment When Using Multiple Antennas," *Wireless Personal Communications*, vol. 6, pp. 311–335, 1998.

[3] A. Goldsmith, S. Jafar, N. Jindal, and S. Vishwanath, "Capacity Limits of MIMO Channels," *IEEE Journal on Selected Areas in Communications*, vol. 21, pp. 684–702, Jun. 2003.

[4] 3GPP Technical Report 25.913, "Requirements for Evolved UTRA (E-UTRA) and Evolved UTRAN (E-UTRAN) (Release 9)." http://www.3gpp.org/ftp/specs/html-info/25913.htm, 2009-12-28.

[5] M. Medard, "The Effect Upon Channel Capacity in Wireless Communications of Perfect and Imperfect Knowledge of the Channel," *IEEE Trans. Information Theory*, vol. 46, pp. 933–946, May 2000.

[6] L. Tong and S. Perreau, "Multichannel Blind Identification: From Subspace to Maximum Likelihood Methods," *Proceedings of the IEEE*, vol. 86, pp. 1951–1968, Oct. 1998.

[7] Y. Hua and M. Wax, "Strict Identifiability of Multiple FIR Channels Driven by an Unknown Arbitrary Sequence," *IEEE Trans. Signal Processing*, vol. 44, pp. 756–759, Mar. 1996.

[8] A. Liavas, P. Regalia, and J.-P. Delmas, "Robustness of Least-Squares and Subspace Methods for Blind Channel Identification/Equalization With Respect to Effective Channel Undermodeling/Overmodeling," *IEEE Trans. Signal Processing*, vol. 47, pp. 1636–1645, Jun. 1999.

[9] S. M. Kay, *Fundamentals of Statistical Signal Processing, Vol. I - Estimation Theory.* Englewood Cliffs, NJ: Prentice Hall, 1993.

[10] A. Hjørungnes and D. Palomar, "Patterned Complex-Valued Matrix Derivatives," in *5th IEEE Sensor Array and Multichannel Signal Processing Workshop, 2008.*, pp. 293–297, July 2008.

[11] A. Hjørungnes and D. Gesbert, "Complex-Valued Matrix Differentiation: Techniques and Key Results," *IEEE Trans. Signal Processing*, vol. 55, pp. 2740–2746, Jun. 2007.

[12] J. Magnus, *Matrix Differential Calculus with Applications in Statistics and Econometrics*. New York, NY, USA: John Wiley & Sons, 1988.

[13] J. Magnus and H. Neudecker, "The Commutation Matrix: Some Properties and Applications," *Annals of Statistics*, vol. 7, no. 2, pp. 381–394, 1979.

[14] D.-S. Shiu, G. Foschini, M. Gans, and J. Kahn, "Fading Correlation and its Effect on the Capacity of Multielement Antenna Systems," *IEEE Trans. Communications*, vol. 48, pp. 502–513, Mar. 2000.